

IW-GAE: Importance weighted group accuracy estimation for improved calibration and model selection in unsupervised domain adaptation

Taejong Joo & Diego Klabjan
Department of Industrial Engineering & Management Sciences
Northwestern University
Evanston, IL, USA
{taejong.joo,d-klabjan}@northwestern.edu

Abstract

Reasoning about a model’s accuracy on a test sample from its confidence is a central problem in machine learning, being connected to important applications such as uncertainty representation, model selection, and exploration. While these connections have been well-studied in the i.i.d. settings, distribution shifts pose significant challenges to the traditional methods. Therefore, model calibration and model selection remain challenging in the unsupervised domain adaptation problem—a scenario where the goal is to perform well in a distribution shifted domain without labels. In this work, we tackle difficulties coming from distribution shifts by developing a novel importance weighted group accuracy estimator. Specifically, we formulate an optimization problem for finding an importance weight that leads to an accurate group accuracy estimation in the distribution shifted domain with theoretical analyses. Extensive experiments show the effectiveness of group accuracy estimation on model calibration and model selection. Our results emphasize the significance of group accuracy estimation for addressing challenges in unsupervised domain adaptation, as an orthogonal improvement direction with improving transferability of accuracy.

1 Introduction

In this work, we consider a classification problem in unsupervised domain adaptation (UDA). UDA aims to transfer knowledge from a source domain with ample labeled data to enhance the performance in a target domain where labeled data is unavailable. In UDA, the source and target domains have *different data generating distributions*, so the core challenge is to transfer knowledge contained in the labeled dataset in the source domain to the target domain under the distribution shifts. Over the decades, significant improvements in the transferability from source to target domains have been made, resulting in areas like domain alignment (Ben-David et al., 2010; Ganin et al., 2016; Long et al., 2018; Zhang et al., 2019) and self-training (Cai et al., 2021; Chen et al., 2020; Liu et al., 2021).

Improving calibration performance, which is about matching predictions regarding a random event to the long-term occurrence of the event (Dawid, 1982), is of central interest in the machine learning community due to its significance to safe and trustworthy deployment of machine learning models in critical real-world decision-making systems (Amodei et al., 2016; Lee and See, 2004). In independent and identically distributed (i.i.d.) settings, calibration performance has been significantly improved by various approaches (Gal and Ghahramani, 2016; Guo et al., 2017; Lakshminarayanan et al., 2017). However, producing well-calibrated predictions in UDA remains challenging due to the distribution shifts. Specifically, Wang et al. (2020) show the discernible compromise in calibration performance as an offset against the enhancement of target accuracy. A further observation reveals that state-of-the-art calibrated classifiers in the i.i.d. settings begin to generate unreliable uncertainty representation in the face of distributional shifts (Ovadia et al., 2019). As such, enhancing the calibration performance in UDA requires carefully addressing the impacts of the distribution shifts.

Moreover, the model selection task in UDA remains challenging due to the scarcity of labeled target domain data that are required to evaluate model performance. In the i.i.d. settings, a standard approach for model selection is a cross-validation method—constructing a hold-out dataset for selecting the model that yields the best performance on the hold-out dataset. While cross-validation provides favorable

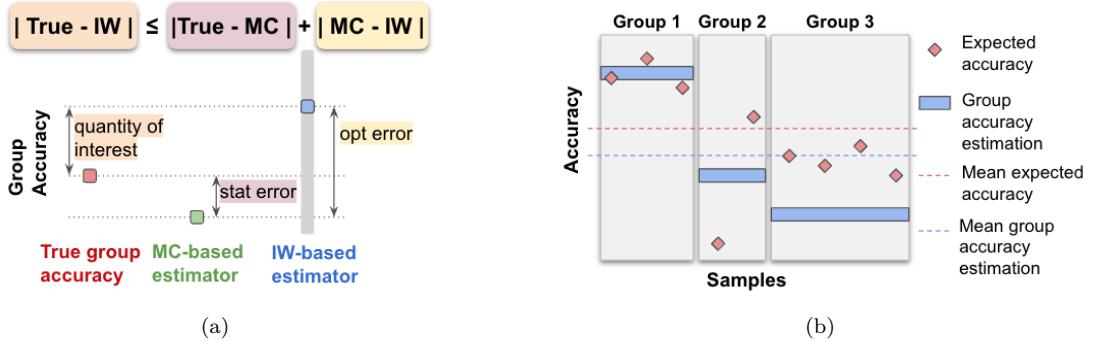


Figure 1: Figure 1(a) illustrates the idea of encouraging two estimators of the source group accuracy close to each other. The shaded areas for the IW-based estimator represent possible estimations under different IW values in the confidence interval of the IW. We show that the quantity of interest—the error of the IW-based estimator—is reduced by optimization in Section 4.1, which can also *reduce its target group accuracy estimation error*. Figure 1(b) illustrates the idea of estimating the group accuracy for model calibration and model selection. Nine data points are assigned to three groups. For the model calibration task, group 1 corresponds to the ideal case where the group accuracy well represents the expected accuracy of the individual samples in the group. However, group 2 has a high discrepancy between expected accuracies of the samples in the group. In this case, even though the group accuracy estimation is correct, the group accuracy estimation is not favorable for model calibration. We prevent this case by group construction developed in Section 4.2. Conversely, group 3 has a small variance of the expected accuracy within the samples in the group. However, the estimator is not appropriate for the model calibration task due to its high bias, which we prevent by solving the novel optimization problem developed in Section 4.1. For the model selection task, we aim to match mean group accuracy estimation (the blue dotted line) to the mean expected accuracy (the red dotted line), which can be induced by accurate group accuracy estimations for each group.

statistical guarantees (Kohavi et al., 1995; Stone, 1977), such guarantees falter in the presence of the distribution shifts due to the violation of the i.i.d. assumption. In practice, it has also been observed that performances of machine learning models measured in one domain have significant discrepancy to their performances in another distribution shifted domain (Hendrycks and Dietterich, 2019; Ovadia et al., 2019; Recht et al., 2019). Therefore, applying model selection techniques in the i.i.d. settings to the labeled source domain is suboptimal in the target domain.

This paper proposes **importance weighted group accuracy estimation (IW-GAE)** that *simultaneously addresses these critical aspects in UDA* from a new perspective of predicting a group accuracy (see Figure 1 for the graphical illustration). We partition predictions into a set of groups and then estimate the group accuracy—the average accuracy of predictions in a group—by importance weighting. When *the group accuracy estimate accurately represents the expected accuracy* of a model for individual samples in the group, using the group accuracy estimate as prediction confidence induces a well-calibrated classifier. When *the average of the group accuracy estimates matches the expected accuracy*, the average group accuracy becomes a good model selection criterion (cf. Figure 1(b)). In this work, we formulate a novel optimization problem for finding importance weights (IW) that induce a group accuracy estimator satisfying these ideal properties under the distribution shifts. Specifically, we define two estimators for *the group accuracy in the source domain*, where only one of them depends on the IW. Then, we find the IW that makes the two estimators close to each other by solving the optimization problem (cf. Figure 1(a)). Through a theoretical analysis and several experiments, we show that the optimization process results in *an accurate group accuracy estimator for the target domain*, thereby improving model calibration and model selection performances.

Our contributions can be summarized as follows: 1) We propose a novel optimization problem for IW estimation that can directly reduce an error of the quantity of interests in UDA with a theoretical analysis; 2) We show when and why considering group accuracy, instead of the accuracy for individual samples, is statistically favorable based on the bias-variance decomposition of the group accuracy estimation error, which can simultaneously benefit model calibration and model selection; 3) On average, IW-GAE improves state-of-the-art by 26% in the model calibration task and 14% in the model selection task.

2 Related work

Model calibration in the i.i.d. settings In a classification problem, the maximum value of the softmax output is often considered as a confidence of a neural network’s prediction. In Guo et al. (2017), it is shown that the modern neural networks are poorly calibrated, tending to produce larger confidences than their accuracies. Based on this observation, Guo et al. (2017) introduce a post-processing approach that adjusts a temperature parameter of the softmax function for adjusting the overall confidence level. In Bayesian approaches (such as Monte-Carlo dropout (Gal and Ghahramani, 2016; Gal et al., 2017), deep ensemble (Lakshminarayanan et al., 2017; Rahaman et al., 2021), and a last-layer Bayesian approach (Joo et al., 2020; Sensoy et al., 2018)), the confidence level adjustment is induced by posterior inference and model averaging. While both post-hoc calibration methods and Bayesian methods have been achieving impressive calibration performances in the i.i.d. setting (Ebrahimi et al., 2020; Maddox et al., 2019; Ovadia et al., 2019), it has been shown that most of the calibration improvement methods fall short under distribution shifts (Ovadia et al., 2019).

Model calibration in UDA While handling model calibration problems under general distribution shifts is challenging, the availability of unlabelled samples in the distribution shifted target domain relaxes the difficulty in UDA. In particular, unlabeled samples in the target domain enable an IW formulation for the quantity of interests in the shifted domain. Therefore, the post-doc calibration methods (e.g., Guo et al. (2017)) can be applied by reweighting calibration measures such as the expected calibration error (Wang et al., 2020) and the Brier score (Park et al., 2020) in the source dataset with an IW. However, estimating the IW brings another difficulty of high-dimensional density estimation. In this work, instead of concentrating on obtaining accurate importance weighted calibration measures for matching the maximum softmax output to the expected accuracy, we aim to directly estimate the accuracy in the distribution shifted target domain.

Model selection in UDA A standard procedure for model selection in the i.i.d. settings is the cross-validation, which enjoys favorable statistical guarantees about bias and variance of model performance (Efron and Tibshirani, 1997; Kohavi et al., 1995; Stone, 1977). However, in UDA, the distribution shifts violate assumptions for the statistical guarantees. Furthermore, in practice, the accuracy measured in one domain is significantly changed in the face of natural/adversarial distribution shifts (Goodfellow et al., 2015; Hendrycks and Dietterich, 2019; Ovadia et al., 2019). To tackle the distribution shift problem, importance weighted cross validation (Sugiyama et al., 2007) applies importance sampling for obtaining an unbiased estimate of model performance in the distribution shifted target domain. Further, recent work in UDA controls variance of the importance-weighted cross validation with a control variate (You et al., 2019). These methods aim to accurately estimate the IW and then use an IW formula for the expected accuracy estimation. In this work, our method concerns the accuracy estimation error in the target domain during the process of IW estimation, which can potentially induce an IW estimation error but resulting in an accurate accuracy estimator.

3 Background

Notation and problem setup Let $\mathcal{X} \subseteq \mathbb{R}^r$ and $\mathcal{Y} = [K] := \{1, 2, \dots, K\}$ be input and label spaces. Let $\hat{Y} : \mathcal{X} \rightarrow [K]$ be the prediction function of a model and $Y(x)$ is a (conditional) K -dimensional categorical random variable related to a label at $X = x$. When there is no ambiguity, we represent $Y(x)$ and $\hat{Y}(x)$ as Y and \hat{Y} for brevity. We are given a labeled source dataset $\mathcal{D}_S = \{(x_i^{(S)}, y_i^{(S)})\}_{i=1}^{N^{(S)}}$ sampled from $p_{S_{XY}}$ and an unlabeled target dataset $\mathcal{D}_T = \{x_i^{(T)}\}_{i=1}^{N^{(T)}}$ sampled from p_{T_X} where $p_{S_{XY}}$ is a joint data generating distribution of the source domain and p_{T_X} is a marginal data generating distribution of the target domain. We also denote $\mathbb{E}_p[\cdot]$ as the population expectation and $\hat{\mathbb{E}}_p[\cdot]$ as its empirical counterpart. For $p_{S_{XY}}$ and $p_{T_{XY}}$, we consider a covariate shift without a concept shift; i.e., $p_{S_X}(x) \neq p_{T_X}(x)$ but $p_{S_{Y|X}}(y|x) = p_{T_{Y|X}}(y|x)$ for all $x \in \mathcal{X}$. For the rest of the paper, we use the same notation for marginal and joint distributions when there is no ambiguity; that is, $\mathbb{E}_{p_S}[u_1(X)] = \mathbb{E}_{p_{S_X}}[u_1(X)]$ and $\mathbb{E}_{p_S}[u_2(X, Y)] = \mathbb{E}_{p_{S_{XY}}}[u_2(X, Y)]$. However, we use the explicit notation for the conditional distribution as $p_{S_{Y|X}}$ and $p_{T_{Y|X}}$ to avoid confusion.

In this work, we consider an IW estimation problem for improving model calibration and model selection in UDA. Importance weighting can address many problems in UDA due to its statistical exactness for dealing with two different probability distributions under the absolute continuity condition (Horvitz and

Thompson, 1952; Sugiyama et al., 2007) that is often assumed in the literature. Specifically, for densities p_S and p_T , a quantity of interest $u(\cdot, \cdot)$ in p_T can be computed by $\mathbb{E}_{p_T}[u(X, Y)] = \mathbb{E}_{p_S}[w^*(X)u(X, Y)]$ where $w^*(x) := \frac{p_T(x)}{p_S(x)}$ is the IW of x . We next review two main approaches for IW estimation, which circumvent the challenges of directly estimating the IW, or the densities p_S and p_T , in a high-dimensional space.

Estimating IW by discriminative learning Bickel et al. (2007) formulate IW estimation as a discriminative learning problem by applying the Bayes' rule, which is more sample efficient (Long and Servedio, 2006; Ng and Jordan, 2001; Tu, 2007). Specifically, with a discriminative model that classifies source and target samples, the IW can be computed as $w^*(x) = \frac{p_T(x)}{p_S(x)} = \frac{\nu(x|d=1)}{\nu(x|d=0)} = \frac{P(d=0)P(d=1|x)}{P(d=1)P(d=0|x)}$ where ν is a distribution over $(x, d) \in (\mathcal{X} \times \{0, 1\})$ and d is a Bernoulli random variable indicating whether x belongs to the target domain or not. For IW estimation, $P(d=0)/P(d=1)$ can be estimated by counting sample sizes of \mathcal{D}_S and \mathcal{D}_T . Also, to estimate $P(d=1|x)/P(d=0|x)$, a logistic regression model can be trained by assigning a domain index of zero to $x_S \in \mathcal{D}_S$ and one to $x_T \in \mathcal{D}_T$, and maximizing log-likelihood with respect to the domain datasets.

Estimating confidence interval of importance weight Recently, nonparametric estimation of the IW is proposed in the context of generating a probably approximately correct (PAC) prediction set (Park et al., 2022). In this approach, \mathcal{X} is partitioned into B number of bins ($\mathcal{X} = \cup_{i=1}^B \mathcal{B}_i$) with

$$I^{(B)} : \mathcal{X} \rightarrow [B] \text{ such that } \mathcal{B}_i = \{x \in \mathcal{X} | I^{(B)}(x) = i\}, \quad i \in [B]. \quad (1)$$

Then, confidence intervals (CIs) of the binned probabilities $\bar{p}_S(x) = \bar{p}_{S_{I^{(B)}(x)}}$ with $\bar{p}_{S_j} = \int_{\mathcal{B}_j} p_S(x) dx$ and $\bar{p}_T(x) = \bar{p}_{T_{I^{(B)}(x)}}$ with $\bar{p}_{T_j} = \int_{\mathcal{B}_j} p_T(x) dx$ are constructed. Specifically, for \bar{p}_{S_j} , the number of samples in a bin $n_j^{(S)} := \sum_{i=1}^{N^{(S)}} \mathbf{1}(x_i^{(S)} \in \mathcal{B}_j)$ is interpreted as a sample from $\text{Binom}(N^{(S)}, \bar{p}_{S_j})$. Then, the Clopper–Pearson CI (Clopper and Pearson, 1934) provides the CI of \bar{p}_{S_j} as $\underline{\theta}_S(n_j^{(S)}; N^{(S)}, \delta/2) \leq \bar{p}_{S_j} \leq \bar{\theta}_S(n_j^{(S)}; N^{(S)}, \delta/2)$ with probability at least $1 - \delta$ where $\bar{\theta}(k; m, \delta) := \inf\{\theta \in [0, 1] | F(k; m, \theta) \leq \delta\}$ and $\underline{\theta}(k; m, \delta) := \sup\{\theta \in [0, 1] | F(k; m, \theta) \geq \delta\}$ with F being the cumulative distribution function of the binomial distribution. Similarly, we can obtain the CIs of \bar{p}_{T_j} by collecting $n_j^{(T)} := \sum_{i=1}^{N^{(T)}} \mathbf{1}(x_i^{(T)} \in \mathcal{B}_j)$ and following the same procedure, which are denoted as $\underline{\theta}_T(n_j^{(T)}; N^{(T)}, \delta/2)$ and $\bar{\theta}_T(n_j^{(T)}; N^{(T)}, \delta/2)$.

With the CIs of p_{S_j} and p_{T_j} for $j \in [B]$, the CI of the IW in \mathcal{B}_j can be obtained. Specifically, for $\bar{\delta} := \delta/2B$, the following inequality holds with probability at least $1 - \delta$ (Park et al., 2022):

$$\frac{[\underline{\theta}_T(n_j^{(T)}; N^{(T)}, \bar{\delta}) - G]^+}{\bar{\theta}_S(n_j^{(S)}; N^{(S)}, \bar{\delta}) + G} \leq w_j^* := \frac{\bar{p}_{T_j}}{\bar{p}_{S_j}} \leq \frac{\bar{\theta}_T(n_j^{(T)}; N^{(T)}, \bar{\delta}) + G}{[\underline{\theta}_S(n_j^{(S)}; N^{(S)}, \bar{\delta}) - G]^+} \quad (2)$$

where $G \in \mathbb{R}_+$ is a constant that satisfies $\int_{\mathcal{B}_j} |p_S(x) - p_S(x')| dx' \leq G$ and $\int_{\mathcal{B}_j} |p_T(x) - p_T(x')| dx' \leq G$ for all $x \in \mathcal{B}_j$ and $j \in [B]$. For the rest of the paper, we refer to $\{w_i^*\}_{i \in B}$ as **binned IWs**. Also, we let $\Phi_j := \left[\frac{[\underline{\theta}_T(n_j^{(T)}; N^{(T)}, \bar{\delta}) - G]^+}{\bar{\theta}_S(n_j^{(S)}; N^{(S)}, \bar{\delta}) + G}, \frac{\bar{\theta}_T(n_j^{(T)}; N^{(T)}, \bar{\delta}) + G}{[\underline{\theta}_S(n_j^{(S)}; N^{(S)}, \bar{\delta}) - G]^+} \right]$ be the CI of w_j^* .

4 Importance weighted group accuracy estimation

In this section, we propose IW-GAE that estimates the group accuracy in the target domain for addressing model calibration and selection tasks in UDA. Specifically, we construct M groups denoted by $\{\mathcal{G}_i\}_{i \in [M]}$ and then estimate the average accuracy of each group in the target domain with an IW. To this end, we define the **target group accuracy** of a group \mathcal{G}_n with the true IW w^* as

$$\alpha_T(\mathcal{G}_n; w^*) := \mathbb{E}_{p_S} \left[w^*(X) \mathbf{1}(Y = \hat{Y}) | X \in \mathcal{G}_n \right] \frac{P(X_S \in \mathcal{G}_n)}{P(X_T \in \mathcal{G}_n)} \quad (3)$$

where X_S and X_T are random variables having densities p_S and p_T , respectively. It is called the group accuracy because $\mathbb{E}_{p_S} \left[w^*(X) \mathbf{1}(Y = \hat{Y}) | X \in \mathcal{G}_n \right] \frac{P(X_S \in \mathcal{G}_n)}{P(X_T \in \mathcal{G}_n)} = \int_{x \in \mathcal{X}} \mathbf{1}(Y = \hat{Y}) \frac{p_T(x) \mathbf{1}(x \in \mathcal{G}_n)}{P(X_T \in \mathcal{G}_n)} dx = \mathbb{E}_{p_T} \left[\mathbf{1}(Y(X) = \hat{Y}(X)) | X \in \mathcal{G}_n \right]$. We denote $\hat{\alpha}_T(\mathcal{G}_n; w^*)$ to be the expectation with respect to the empirical measure. In Appendix B.1, we present a sufficient condition that the group accuracy estimator is better

than the individual accuracy estimator under a relatively loose condition of group constructions. We also define the **source group accuracy** as

$$\alpha_S(\mathcal{G}_n; w^*) := \mathbb{E}_{p_T} \left[\frac{\mathbf{1}(Y(X) = \hat{Y}(X))}{w^*(X)} \middle| X \in \mathcal{G}_n \right] \frac{P(X_T \in \mathcal{G}_n)}{P(X_S \in \mathcal{G}_n)}. \quad (4)$$

In the following, we explain IW estimation and group construction for estimating the group accuracy. We denote an estimate for group accuracy with an estimated IW $\hat{w} : \mathcal{X} \rightarrow \mathbb{R}_+$ and a group assignment $I^{(g)} : \mathcal{X} \rightarrow [M]$ as $\hat{\alpha}_T(\mathcal{G}_i; \hat{w})$ with $\mathcal{G}_i = \{x \in \mathcal{X} : I^{(g)}(x) = i\}$ for $i \in [M]$. We discuss how to obtain \hat{w} in Section 4.1 and $I^{(g)}$ in Section 4.2, respectively.

After obtaining \hat{w} and $I^{(g)}$, $\hat{\alpha}_T(\mathcal{G}_i; \hat{w})$ can be used to perform the following tasks: **1) Model calibration:** For a test sample $x \sim p_T$, $\hat{\alpha}_T(\mathcal{G}_{I^{(g)}(x)}; \hat{w})$ provides an estimate of confidence, which is preferably close to $\mathbb{E}_{p_{T_Y|x}}[\mathbf{1}(Y(x) = \hat{Y}(x))]$; **2) Model selection:** For a validation dataset from the target domain \mathcal{D}_T , we compare models based on $\hat{\mathbb{E}}_{p_T}[\hat{\alpha}_T(\mathcal{G}_{I^{(g)}(X)}; \hat{w})]$.

4.1 Importance weight estimation

Our goal is to obtain IW \hat{w} that leads to $\alpha_T(\mathcal{G}_n; w^*) \approx \alpha_T(\mathcal{G}_n; \hat{w})$ for $n \in [M]$. The proposed method is based on a CI estimation method developed for producing the PAC prediction set discussed in Section 3 (Park et al., 2022)¹. Specifically, given the CI of binned IWs $\{\Phi_i\}_{i \in [B]}$ in (2), our goal is to find binned IWs $\{w_i \in \Phi_i\}_{i \in [B]}$ that give an accurate group accuracy estimation. We let $\tilde{w}(x) := w_{I^{(B)}(x)}$ be the induced IW estimation from binned IWs where $I^{(B)}$ is the partition in (1).

Our idea for accurately estimating the ‘‘target’’ group accuracy with IW estimator \tilde{w} is to define two estimators for the ‘‘source’’ group accuracy defined in (4), with one estimator dependent on a target accuracy estimate, and to encourage the two estimators to agree with each other. This approach can be validated because *the target accuracy estimation error of \tilde{w} can be upper bounded by its source accuracy estimation error* (see Appendix E.7 for empirical analyses); that is,

$$\begin{aligned} |\alpha_T(\mathcal{G}_n; w^*) - \alpha_T(\mathcal{G}_n; \tilde{w})| &= \left| \mathbb{E}_{p_T} \left[\tilde{w}(X) \left(\frac{1}{w^*(X)} - \frac{1}{\tilde{w}(X)} \right) \mathbf{1}(Y = \hat{Y}) \middle| X \in \mathcal{G}_n \right] \frac{P(X_S \in \mathcal{G}_n)}{P(X_T \in \mathcal{G}_n)} \right. \\ &\quad \left. \leq \bar{M} \cdot |\alpha_S(\mathcal{G}_n; w^*) - \alpha_S(\mathcal{G}_n; \tilde{w})| \left(\frac{P(X_T \in \mathcal{G}_n)}{P(X_S \in \mathcal{G}_n)} \right)^2 \right. \end{aligned} \quad (5)$$

where $\bar{M} = \max_{x \in \text{Supp}(p_T)} \tilde{w}(x)$ and $\alpha_S(\mathcal{G}_n; \tilde{w})$ is obtained by replacing w^* with \tilde{w} in (4).

To develop the first estimator, note that we can reliably approximate the source group accuracy with \mathcal{D}_S by Monte-Carlo estimation with the error of $\mathcal{O}(1/\sqrt{|\mathcal{G}_n(\mathcal{D}_S)|})$ where $\mathcal{G}_n(\mathcal{D}_S) := \{(x_k, y_k) \in \mathcal{D}_S : x_k \in \mathcal{G}_n\}$; we denote the Monte-Carlo estimate as $\hat{\alpha}_S^{(MC)}(\mathcal{G}_n) = \hat{\mathbb{E}}_{p_S}[\mathbf{1}(Y = \hat{Y}) | X \in \mathcal{G}_n]$.

Based on (4), we define a second estimator for $\alpha_S(\mathcal{G}_i; w^*)$, as a function of binned IWs $\{w_i\}_{i \in [B]}$, by assuming $\mathbb{E}_{p_{T_Y|x}}[\mathbf{1}(Y(x) = \hat{Y}(x))] = \hat{\alpha}_T(\mathcal{G}_n; \{w_i\}_{i \in [B]})$ for all $x \in \mathcal{G}_n$:

$$\begin{aligned} \hat{\alpha}_S^{(IW)}(\mathcal{G}_n; \{w_i\}_{i \in [B]}) &:= \frac{\hat{P}(X_T \in \mathcal{G}_n)}{\hat{P}(X_S \in \mathcal{G}_n)} \cdot \hat{\mathbb{E}}_{p_T} \left[\frac{\hat{\alpha}_T(\mathcal{G}_n; \{w_i\}_{i \in [B]})}{\tilde{w}(X)} \middle| X \in \mathcal{G}_n \right] \\ &= \hat{\mathbb{E}}_{p_T} \left[\frac{1}{\tilde{w}(X)} \middle| X \in \mathcal{G}_n \right] \hat{\mathbb{E}}_{p_S} \left[\mathbf{1}(Y = \hat{Y}) \tilde{w}(X) \middle| X \in \mathcal{G}_n \right] \end{aligned} \quad (6)$$

where $\hat{\alpha}_T(\mathcal{G}_n; \{w_i\}_{i \in [B]})$ is an empirical estimate of the target accuracy with $\{w_i\}_{i \in [B]}$ in (3), $\hat{P}(X_T \in \mathcal{G}_n) := \hat{E}_{p_T}[\mathbf{1}(X \in \mathcal{G}_n)]$, and $\hat{P}(X_S \in \mathcal{G}_n) := \hat{E}_{p_S}[\mathbf{1}(X \in \mathcal{G}_n)]$.

We aim to formulate an optimization problem to choose binned IWs from CIs such that

$$\min_{\{w_i \in \Phi_i\}_{i \in [B]}} (\hat{\alpha}_S^{(IW)}(\mathcal{G}_n; \{w_i\}_{i \in [B]}) - \hat{\alpha}_S^{(MC)}(\mathcal{G}_n))^2. \quad (7)$$

However, note that $\hat{\alpha}_S^{(IW)}(\mathcal{G}_n; \{w_i\}_{i \in [B]})$ in (6) is non-convex with respect to w_i ’s (see Appendix A.1 for the derivation), which is in general not effectively solvable with optimization methods (Jain et al., 2017).

¹However, we want to emphasize that IW-GAE can be applied to any valid CI estimators (cf. Appendix B.2).

Therefore, we introduce a relaxed reformulation of (6) by separating binned IWs for source and target, which introduces coordinatewise convexity. Specifically, we redefine the estimator in (6) as

$$\hat{\alpha}_S^{(IW)}(\mathcal{G}_n; \{w_i^{(S)}, w_i^{(T)}\}_{i \in [B]}) := \hat{\mathbb{E}}_{p_T} \left[\frac{1}{\tilde{w}^{(T)}(X)} \middle| X \in \mathcal{G}_n \right] \hat{\mathbb{E}}_{p_S} \left[\mathbf{1}(Y = \hat{Y}) \tilde{w}^{(S)}(X) \middle| X \in \mathcal{G}_n \right] \quad (8)$$

where $\tilde{w}^{(S)}(X) := w_{I^{(S)}(X)}^{(S)}$ and $\tilde{w}^{(T)}(X) := w_{I^{(T)}(X)}^{(T)}$. Then, we encourage agreements of $w_i^{(S)}$ and $w_i^{(T)}$ for $i \in [B]$ through constraints. Specifically, for each group \mathcal{G}_n , we find binned IWs $w^\dagger(n) \in \mathbb{R}_+^{2B}$ by solving the following optimization problem:

$$w^\dagger(n) \in \arg \min_{\{w_i^{(S)}, w_i^{(T)}\}_{i \in [B]}} \left(\hat{\alpha}_S^{(MC)}(\mathcal{G}_n) - \hat{\alpha}_S^{(IW)}(\mathcal{G}_n; \{w_i^{(S)}, w_i^{(T)}\}_{i \in [B]}) \right)^2 \quad (9)$$

$$\text{s.t. } w_i^{(S)} \in \Phi_i, \quad \text{for } i \in [B] \quad (10)$$

$$w_i^{(T)} \in \Phi_i, \quad \text{for } i \in [B] \quad (11)$$

$$\|w_i^{(T)} - w_i^{(S)}\|_2^2 \leq \delta^{(tol)} \quad \text{for } i \in [B] \quad (12)$$

$$\left| \hat{\mathbb{E}}_{p_S}[\tilde{w}^{(S)}(X) | X \in \mathcal{G}_n] - \frac{\hat{P}(X_T \in \mathcal{G}_n)}{\hat{P}(X_S \in \mathcal{G}_n)} \right| \leq \delta^{(prob)} \quad (13)$$

$$\left| \hat{\mathbb{E}}_{p_T}[1/\tilde{w}^{(T)}(X) | X \in \mathcal{G}_n] - \frac{\hat{P}(X_S \in \mathcal{G}_n)}{\hat{P}(X_T \in \mathcal{G}_n)} \right| \leq \delta^{(prob)} \quad (14)$$

where $\delta^{(tol)}$ and $\delta^{(prob)}$ are small constants. Box constraints (10) and (11) ensure that the obtained solution is in the CI, which bounds the estimation error of $w_i^{(S)}$ and $w_i^{(T)}$ by $|\Phi_i|$. This can also bound the target group accuracy estimation error as $|\alpha_T(\mathcal{G}_n; w^*) - \alpha_T(\mathcal{G}_n; \{w_i^{(S)}\}_{i \in [B]})| \leq \max_{b \in [B]} |\Phi_b| P(X_S \in \mathcal{G}_n) / P(X_T \in \mathcal{G}_n)$. Constraint (12) corresponds to the relaxation for removing non-convexity of the original objective, and setting $\delta^{(tol)} = 0$ recovers the original objective. Constraints (13) and (14) are based on the equalities that the true IW $w^*(\cdot)$ satisfies: $\mathbb{E}_{p_S}[w^*(X) | X \in \mathcal{G}_n] = \frac{P(X_T \in \mathcal{G}_n)}{P(X_S \in \mathcal{G}_n)}$ and $\mathbb{E}_{p_T}[1/w^*(X) | X \in \mathcal{G}_n] = \frac{P(X_S \in \mathcal{G}_n)}{P(X_T \in \mathcal{G}_n)}$.

Since the above optimization problem is a constrained nonlinear optimization problem with box constraints, we solve it through sequential least square programming (Kraft, 1988). Note that the objective (9) is convex with respect to the block $(w_1^{(S)}, w_2^{(S)}, \dots, w_B^{(S)})$ and the block $(w_1^{(T)}, w_2^{(T)}, \dots, w_B^{(T)})$, but not jointly convex. Therefore, using a quasi-Newton method can guarantee only convergence to a local optimum (Nocedal and Wright, 1999). Nevertheless, due to constraints (13) and (14), the asymptotic convergence $(w^\dagger(n))_i \rightarrow w_i^*$ and $(w^\dagger(n))_{i+B} \rightarrow w_i^*$ as $N^{(S)} \rightarrow \infty$ and $N^{(T)} \rightarrow \infty$ can be trivially guaranteed because $|\Phi_i| \rightarrow 0$ for $i \in [B]$ (Thulin, 2014). Values $w^\dagger(n)$ depend on $N^{(S)}$ and $N^{(T)}$ but we omit this dependency in the notation.

The above optimization problem can be thought of as aiming to estimate the truncated IW $w(x|X \in \mathcal{G}_n) := \frac{p_T(x|X \in \mathcal{G}_n)}{p_S(x|X \in \mathcal{G}_n)}$ for each \mathcal{G}_n that can induce an accurate source group accuracy estimator. However, the objective in (9) does not measure the source group accuracy estimation error. In the following proposition, we show that the above optimization *minimizes the upper bound of the source group accuracy estimation error*, thereby the target group accuracy estimation error due to (5).

Proposition 4.1 (Upper bound of source group accuracy estimation error). *Let $w^\dagger(n)$ be a solution to the optimization problem for \mathcal{G}_n defined in (9)-(14) with $\delta^{(tol)} = 0$ and $\delta^{(prob)} = 0$. Let $\epsilon_{opt}(w^\dagger(n)) := \left(\hat{\alpha}_S^{(MC)}(\mathcal{G}_n) - \hat{\alpha}_S^{(IW)}(\mathcal{G}_n; w^\dagger(n)) \right)^2$ be the objective value. For $\tilde{\delta} > 0$, the following inequality holds with probability at least $1 - \tilde{\delta}$:*

$$|\alpha_S(\mathcal{G}_n; w^*) - \alpha_S(\mathcal{G}_n; w^\dagger(n))| \leq \epsilon_{opt}(w^\dagger(n)) + \epsilon_{stat} + \text{IdentBias}(w^\dagger(n); \mathcal{G}_n) \quad (15)$$

where $\epsilon_{stat} \in \mathcal{O}(\log(1/\tilde{\delta})/\sqrt{|\mathcal{G}_n(\mathcal{D}_S)|})$ and $\text{IdentBias}(w^\dagger(n); \mathcal{G}_n) =$

$$\frac{P(X_T \in \mathcal{G}_n)}{2P(X_S \in \mathcal{G}_n)} \left(\mathbb{E}_{p_T} \left[(\mathbf{1}(Y(X) = \hat{Y}(X)) - \alpha_T(\mathcal{G}_n; w^*))^2 | X \in \mathcal{G}_n \right] + \frac{1}{w^\dagger(n)^2} \right) \quad (16)$$

for $w^\dagger(n) := \min_{i \in [2B]} \{w_i^\dagger(n)\}$.

The proof is based on the Cauchy-Schwarz inequality, which is provided in Appendix A. Proposition 4.1 shows that we can reduce the source accuracy estimation error by reducing $\epsilon_{opt}(w^\dagger(n))$ and $IdentBias(w^\dagger(n); \mathcal{G}_n)$. In Section 4.2, we deal with the design of $I^{(g)}$ that can reduce this term. Note that the number of groups M could highly influence ϵ_{stat} and $IdentBias(w^\dagger(n); \mathcal{G}_n)$ (see the discussion in Appendix B.3). However, we found that IW-GAE is not sensitive to even large changes in M (cf. Appendix E.6). Also, we empirically analyze the tightness of (15) in Appendix E.7. Finally, for tightening the upper bounds in (5) and (15), we bound the maximum and minimum values of IW, which is a common technique in IW-based estimations (Park et al., 2022; Wang et al., 2020).

4.2 Group construction

In this section, we design a group assignment function $I^{(g)}$ for constructing $\{\mathcal{G}_i\}_{i \in [M]}$ that can lead to an accurate group accuracy estimation. Proposition 4.1 provides the bias of the identical accuracy assumption. Now, we show that $IdentBias(w^\dagger(n); \mathcal{G}_n)$ depends on the bias of the target group accuracy estimator and the variance of prediction correctness within the group.

Proposition 4.2 (Bias-variance decomposition). *Let $\hat{\alpha}_T(\mathcal{G}_n)$ be an estimate for $\alpha_T(\mathcal{G}_n; w^*)$. Then, the bias of the identical accuracy assumption is given by*

$$IdentBias(w^\dagger(n); \mathcal{G}_n) = \frac{P(X_T \in \mathcal{G}_n)}{2P(X_S \in \mathcal{G}_n)} \left(\frac{1}{w^\dagger(n)^2} + Bias(\hat{\alpha}_T(\mathcal{G}_n))^2 + Var(\mathbf{1}(Y = \hat{Y})|\mathcal{G}_n) \right) \quad (17)$$

where $Bias(\hat{\alpha}_T(\mathcal{G}_n)) := |\alpha_T(\mathcal{G}_n; w^*) - \hat{\alpha}_T(\mathcal{G}_n)|$ is the bias of the estimate $\hat{\alpha}_T(\mathcal{G}_n)$ and $Var(\mathbf{1}(Y = \hat{Y})|\mathcal{G}_n) := \mathbb{E}_{p_T} \left(\mathbf{1}(Y = \hat{Y}) - \alpha_T(\mathcal{G}_n; w^*) \right)^2$ is the variance of the correctness of predictions in \mathcal{G}_n .

The proof is similar to the bias-variance decomposition technique in statistics, and we defer it to Appendix A. Proposition 4.2 suggests forming a group having a small variance in the correctness within the group. Further, a lower variance would be beneficial for preventing potential misspecification of the accuracy within a group (cf. Figure 1(b)). Therefore, we group examples by the maximum value of the softmax output based on strong empirical evidence that the maximum value of the softmax output is highly correlated with accuracy (Guo et al., 2017; Wang et al., 2020); i.e., $\mathcal{G}_n(\mathcal{D}) := \{x_i \in \mathcal{D} | \frac{n-1}{M} \leq (\phi(g(x_i)))_j \leq \frac{n}{M}, j \in m(x_i)\}$ for $\mathcal{D} \in \{\mathcal{D}_S, \mathcal{D}_T\}$ and $n \in [M]$ where $g: \mathcal{X} \rightarrow \mathbb{R}^K$ is the logit function of a neural network, ϕ is the K -dimensional softmax function, and $m(x_i) := \arg \max_{k \in [K]} (\phi(g(x_i)))_k$.

In addition, we use a separate criterion for grouping of source and target samples inspired by results that an overall scale of the maximum value of the softmax output significantly varies from one domain to another (Yu et al., 2022). Therefore, we introduce a temperature scale parameter for target samples that adjusts the sharpness of the softmax output for target predictions. This results in the nested optimization of $\min_{t \in \mathcal{T}} \left\{ \text{optimization problem in (9)-(14) with } \mathcal{G}_n(\mathcal{D}_S) \text{ and } \mathcal{G}_n^{(t)}(\mathcal{D}_T) \right\}$ where $\mathcal{G}_n^{(t)}(\mathcal{D}_T) := \{x_i \in \mathcal{D}_T | \frac{n-1}{M} \leq (\phi(g(x_i)/t))_j \leq \frac{n}{M}, j \in m(x_i)\}$ are the samples in \mathcal{G}_n under the temperature-scaled prediction (see Appendix C.1 for the complete optimization form). Based on the facts that a group separation is not sensitive to small changes in the temperature and the inner optimization is not smooth with respect to t , we use a discrete set for \mathcal{T} ; that is, $\mathcal{T} = \{t_1, t_2, \dots, t_n\}$. We note that the inner optimization problem is readily solvable, so the discrete optimization can be performed without much additional computational overhead.

5 Experiments

We evaluate IW-GAE on model calibration and selection tasks. Since both tasks are based on UDA classification tasks, we first provide the common setup and task-specific setup such as the baselines and evaluation metrics in the corresponding sections. For all experiments in this section, we evaluate our method on the popular Office-Home (Venkateswara et al., 2017) dataset, which contains around 15,000 images of 65 categories from four domains (Art, Clipart, Product, Real-World). We also show robustness of our findings by performing a large-scale experiment with the VisDa-2017 (Peng et al., 2017) dataset containing around 280,000 images in Appendix E.1.

A base model is required for implementing the baseline methods and IW-GAE, which serve as the test objectives for the model calibration and selection tasks. We consider maximum mean discrepancy (MDD; (Zhang et al., 2019)) with ResNet-50 (He et al., 2016) as the backbone neural network, which is the most popular high-performing UDA method. MDD aims to learn domain invariant representation

Task	Method	Ar-CI	Ar-Pr	Ar-Rw	Cl-Ar	Cl-Pr	Cl-Rw	Pr-Ar	Pr-CI	Pr-Rw	Rw-Ar	Rw-CI	Rw-Pr	Avg
Model calibration	Vanilla	40.61	25.62	15.56	33.83	25.34	24.75	33.45	38.62	16.76	23.37	36.51	14.01	27.37
	TS	35.86	22.84	10.60	28.24	20.74	20.06	32.47	37.20	14.89	18.36	34.62	12.28	24.01
	CPCS	22.93	22.07	10.19	26.88	18.36	14.05	28.28	29.20	12.06	15.76	26.54	11.14	19.79
	IW-TS	32.63	22.90	11.27	28.05	19.65	18.67	30.77	38.46	15.10	17.69	32.20	11.77	23.26
	TransCal	33.57	20.27	8.88	26.36	18.81	18.42	27.35	29.86	10.48	16.17	29.90	10.00	20.84
	IW-Mid	23.25	31.62	12.99	17.15	18.71	9.23	27.75	30.35	9.02	13.64	26.32	10.60	19.22
	IW-GAE	12.78	4.70	12.93	7.52	4.42	4.11	9.50	17.49	8.40	7.62	9.52	8.14	8.93
	Oracle	10.45	10.72	6.47	8.10	7.62	6.55	11.88	9.39	5.93	7.54	10.72	5.70	8.42
Model selection	Vanilla	53.31	70.96	77.44	59.70	65.17	69.96	57.07	50.95	74.75	68.81	57.11	80.13	65.45
	IWCV	53.24	69.61	72.50	59.70	65.17	67.50	57.07	55.21	74.75	68.81	58.51	80.13	65.18
	DEV	53.31	70.72	77.44	59.79	67.99	69.96	57.07	52.50	77.12	70.50	53.38	82.27	66.00
	IW-Mid	54.13	69.27	78.47	61.48	68.03	71.06	59.99	55.21	78.79	70.50	57.11	83.10	67.26
	IW-GAE	54.34	70.96	78.47	61.48	69.93	71.06	62.79	55.21	78.79	70.50	58.51	83.31	67.95
	Lower bound	52.51	69.27	72.50	59.70	65.17	67.50	57.07	50.95	74.75	68.81	50.90	80.13	64.10
	Oracle	54.34	70.96	78.47	61.48	69.93	71.06	62.79	55.21	78.79	71.32	58.51	83.31	68.01

Table 1: Model calibration and selection benchmark results of MDD with ResNet-50 on Office-Home. We repeat experiments ten times and report the average value. For model calibration, the numbers indicate the mean ECE with boldface for the minimum mean ECE. For model selection, the numbers indicate the mean test accuracy of selected model with boldface for the maximum mean test accuracy. For the model calibration task, Oracle is obtained by applying TS with labeled test samples in the target domain. For the model selection task, Lower bound and Oracle indicate the accuracy of the models with the worst and best test accuracy, respectively.

while learning a classification task in the source domain. In implementation, we use the popular open source project Transfer Learning Library (Jiang et al., 2020). We use the default hyperparameters in all experiments. Further details are explained in Appendix D.

IW estimation is required for implementing baseline methods and construct bins for estimating the CI of the IW. We adopt a linear logistic regression model on top of the neural network’s representation as the discriminative learning-based estimation, following Wang et al. (2020). Specifically, it first upsamples from one domain to make $|\mathcal{D}_S| = |\mathcal{D}_T|$, and then it labels samples with the domain index: $\{(h(x), 1) | x \in \mathcal{D}_T\}$ and $\{(h(x), 0) | x \in \mathcal{D}_S\}$ where h is the feature map of the neural network. Then, logistic regression is trained with a quasi-Newton method until convergence.

5.1 Model calibration performance

Setup & Metric In this experiment, our goal is to match the confidence of a prediction to its expected accuracy in the target domain. Following the standard (Guo et al., 2017; Park et al., 2020; Wang et al., 2020), we use expected calibration error (ECE) on the test dataset as a measure of calibration performance. The ECE measures the average absolute difference between the confidence and accuracy of binned groups, which is defined as $ECE(\mathcal{D}_T) = \sum_{n=1}^m \frac{|\mathcal{G}_n|}{|\mathcal{D}_T|} |\hat{\text{Acc}}(\mathcal{G}_n(\mathcal{D}_T)) - \hat{\text{Conf}}(\mathcal{G}_n(\mathcal{D}_T))|$ where $\hat{\text{Acc}}(\mathcal{G}_n(\mathcal{D}_T))$ is the average accuracy in $\mathcal{G}_n(\mathcal{D}_T)$ and $\hat{\text{Conf}}(\mathcal{G}_n(\mathcal{D}_T))$ is the average confidence in $\mathcal{G}_n(\mathcal{D}_T)$. We use $M = 15$ following the standard value (Guo et al., 2017; Wang et al., 2020).

Baselines We consider the following five different baselines: The *vanilla* method uses a maximum value of the softmax output as the confidence of the prediction. We also consider temperature scaling-based methods that adjust the temperature parameter by maximizing the following calibration measures: *Temperature scaling (TS)* (Guo et al., 2017): the log-likelihood on the source validation dataset; *IW temperature scaling (IW-TS)*: the log-likelihood on the importance weighted source validation dataset; *Calibrated prediction with covariate shift (CPCS)*: the Brier score (Brier, 1950) on the importance weighted source validation dataset; *TransCal* (Wang et al., 2020): the ECE on the importance weighted source validation dataset with a bias and variance reduction technique. These methods also use a maximum value of the (temperature-scaled) softmax output as the confidence.

Results As shown in Table 1, IW-GAE achieves the best average ECEs across different base models. For individual domains, IW-GAE achieves the best ECE among 11 out of the 12 cases. We note that IW-Mid, which selects the middle point in the CI as IW estimation and originates herein, is a strong baseline, outperforming other baselines. IW-GAE improves this strong baseline for every case. This shows that the process of reducing $\epsilon_{opt}(w^\dagger(n))$ reduces the group accuracy estimation error in the target domain, which is consistent with the result in Proposition 4.1.

5.2 Model Selection

Setup & Metric In this experiment, we perform model selection for choosing the best hyperparameter. To this end, we repeat training the MDD method by changing its key hyperparameter of margin coefficient from 1 to 8 (the default value is 4). After training several models under different values of the margin coefficient, we choose one model based on a model selection criterion. For evaluation, we compare the test target accuracy of the chosen model under different model selection methods.

Baselines We consider three baselines that evaluate the model’s performance in terms of the following criterion: *Vanilla*: the minimum classification error on the source validation dataset; *Importance weighted cross validation (IWCV)* (Sugiyama et al., 2007): the minimum importance-weighted classification error on the source validation dataset; *Deep embedded validation (DEV)* (You et al., 2019): the minimum deep embedded validation risk on the source validation dataset.

Results Table 1 shows that model selection with IW-GAE achieves the best average accuracy, improving state-of-the-art by 18% in terms of the relative scale of lower and upper bounds of accuracy. Specifically, IW-GAE achieves the best performance in all cases. We also note that IW-Mid performs the model selection task surprisingly well. This means that, on average, the true IW could be located near the middle point of the CI, while the exact location varies from one group to another.

Note that plain IWCV does not improve the vanilla method on average, which could be due to the inaccurate estimation of the IW by the discriminative learning-based approach. In this sense, IW-GAE has an advantage of depending less on the performance of the IW estimator since the estimated value is used to construct bins for the CI, and then the exact value is found by solving the separate optimization problem. We also remark that our experimental results reveal *dangers of the current practice of using the vanilla method or IWCV in model selection in UDA*.

5.3 Additional experiments

To more rigorously evaluate IW-GAE, we perform the following additional experiments and analyze the results in Appendix E. We apply IW-GAE to a different base model called conditional adversarial domain adaptation (CDAN; (Long et al., 2018)) in E.2. For these experiments, IW-GAE improves state-of-the-art performances by 21% and 2%, respectively. In Appendix E.3, we perform another model selection task of choosing the best checkpoint, and IW-GAE improves the state-of-the-art performance by 9%. In Appendix E.4, we qualitatively evaluate IW-GAE by visually comparing the group accuracy estimation and the average group accuracy, which shows an accurate estimation ability of IW-GAE. In Appendix E.5, we show that the group construction criterion and nested optimization with temperature scaling developed in Section 4.2 work effectively for IW-GAE. In Appendix E.6, a sensitivity analysis shows that IW-GAE consistently performs well even under large changes in the number of bins B and the number of accuracy groups M . In Appendix E.7, we analyze $\epsilon_{opt}(w^\dagger(n))$, $IdentBias(w^\dagger(n); \mathcal{G}_n)$, and their impacts on source and target group accuracy estimation errors. The analysis shows a strong correlation between the target and source group accuracy estimation errors. In addition, we found that $\epsilon_{opt}(w^\dagger(n))$ is strongly correlated with the source group accuracy estimation error. These results support the idea of minimizing $\epsilon_{opt}(w^\dagger(n))$ for obtaining an accurate target group accuracy estimator.

6 Conclusion

In this work, we formulate an optimization problem to choose IW estimation from its CI for accurately estimating group accuracy. Specifically, we define a Monte-Carlo estimator and an IW-based estimator of group accuracy in the source domain and find the IW that makes the two estimators close to each other. Solving the optimization problem not only *reduces the source group accuracy estimation error* but also *leads to an accurate group accuracy estimation in the target domain*. We show that our method achieves state-of-the-art performances in both model calibration and selection tasks in UDA across a wide range of benchmark problems. We believe that the impressive performance gains by our method show a promising future direction of research, which is orthogonal to improving the transferability of accuracy—the main focus in the UDA literature. Finally, we remark that applying IW-GAE and other baselines to the large-language models (XLM-R (Conneau et al., 2019) and GPT-2 (Solaiman et al., 2019)) did not result in improvements. We conjecture that the pre-trained large-language model is less subject to

the distribution shifts, so applying the methods in the i.i.d. settings can serve as a strong baseline. We leave this as an important future direction of research.

Acknowledgement

We would like to thank Jihyeon Hyeong, Yuchen Lou, and Jiezhong Wu for insightful discussions and helpful suggestions in writing the manuscript.

References

- Amodei, D., Olah, C., Steinhardt, J., Christiano, P., Schulman, J., and Mané, D. (2016). Concrete problems in AI safety. *arXiv preprint arXiv:1606.06565*.
- Ben-David, S., Blitzer, J., Crammer, K., Kulesza, A., Pereira, F., and Vaughan, J. W. (2010). A theory of learning from different domains. *Machine Learning*, 79:151–175.
- Bhatia, R. and Davis, C. (2000). A better bound on the variance. *The American Mathematical Monthly*, 107(4):353–357.
- Bickel, S., Brückner, M., and Scheffer, T. (2007). Discriminative learning for differing training and test distributions. In *International Conference on Machine Learning*.
- Brier, G. W. (1950). Verification of forecasts expressed in terms of probability. *Monthly Weather Review*, 78(1):1–3.
- Cai, T., Gao, R., Lee, J., and Lei, Q. (2021). A theory of label propagation for subpopulation shift. In *International Conference on Machine Learning*.
- Chen, Y., Wei, C., Kumar, A., and Ma, T. (2020). Self-training avoids using spurious features under domain shift. In *Advances in Neural Information Processing Systems*.
- Clopper, C. J. and Pearson, E. S. (1934). The use of confidence or fiducial limits illustrated in the case of the binomial. *Biometrika*, 26(4):404–413.
- Conneau, A., Khandelwal, K., Goyal, N., Chaudhary, V., Wenzek, G., Guzmán, F., Grave, E., Ott, M., Zettlemoyer, L., and Stoyanov, V. (2019). Unsupervised cross-lingual representation learning at scale. *arXiv preprint arXiv:1911.02116*.
- Dawid, A. P. (1982). The well-calibrated Bayesian. *Journal of the American Statistical Association*, 77(379):605–610.
- Ebrahimi, S., Elhoseiny, M., Darrell, T., and Rohrbach, M. (2020). Uncertainty-guided continual learning with Bayesian neural networks. In *International Conference on Learning Representations*.
- Efron, B. and Tibshirani, R. (1997). Improvements on cross-validation: the 632+ bootstrap method. *Journal of the American Statistical Association*, 92(438):548–560.
- Gal, Y. and Ghahramani, Z. (2016). Dropout as a Bayesian approximation: Representing model uncertainty in deep learning. In *International Conference on Machine Learning*, pages 1050–1059.
- Gal, Y., Hron, J., and Kendall, A. (2017). Concrete dropout. In *Advances in Neural Information Processing Systems*.
- Ganin, Y., Ustinova, E., Ajakan, H., Germain, P., Larochelle, H., Laviolette, F., Marchand, M., and Lempitsky, V. (2016). Domain-adversarial training of neural networks. *Journal of Machine Learning Research*, 17(1):2096–2030.
- Goodfellow, I. J., Shlens, J., and Szegedy, C. (2015). Explaining and harnessing adversarial examples. In *International Conference on Learning Representations*.
- Guo, C., Pleiss, G., Sun, Y., and Weinberger, K. Q. (2017). On calibration of modern neural networks. In *International Conference on Machine Learning*.
- He, K., Zhang, X., Ren, S., and Sun, J. (2016). Deep residual learning for image recognition. In *IEEE Conference on Computer Vision and Pattern Recognition*.
- Hendrycks, D. and Dietterich, T. (2019). Benchmarking neural network robustness to common corruptions and perturbations. In *International Conference on Learning Representations*.
- Horvitz, D. G. and Thompson, D. J. (1952). A generalization of sampling without replacement from a finite universe. *Journal of the American Statistical Association*, 47(260):663–685.
- Jain, P., Kar, P., et al. (2017). Non-convex optimization for machine learning. *Foundations and Trends® in Machine Learning*, 10(3-4):142–363.
- Jiang, J., Chen, B., Fu, B., and Long, M. (2020). Transfer-learning-library. <https://github.com/thuml/Transfer-Learning-Library>.

- Joo, T., Chung, U., and Seo, M.-G. (2020). Being Bayesian about categorical probability. In *International Conference on Machine Learning*, pages 4950–4961.
- Kohavi, R. et al. (1995). A study of cross-validation and bootstrap for accuracy estimation and model selection. In *International Joint Conferences on Artificial Intelligence*.
- Kraft, D. (1988). A software package for sequential quadratic programming. *Forschungsbericht- Deutsche Forschungs- und Versuchsanstalt für Luft- und Raumfahrt*.
- Lakshminarayanan, B., Pritzel, A., and Blundell, C. (2017). Simple and scalable predictive uncertainty estimation using deep ensembles. In *Advances in Neural Information Processing Systems*.
- Lee, J. D. and See, K. A. (2004). Trust in automation: Designing for appropriate reliance. *Human Factors*, 46(1):50–80.
- Liu, H., Wang, J., and Long, M. (2021). Cycle self-training for domain adaptation. In *Advances in Neural Information Processing Systems*.
- Long, M., Cao, Z., Wang, J., and Jordan, M. I. (2018). Conditional adversarial domain adaptation. In *Advances in Neural Information Processing Systems*.
- Long, P. M. and Servedio, R. A. (2006). Discriminative learning can succeed where generative learning fails. In *Annual Conference on Learning Theory*.
- Maddox, W. J., Izmailov, P., Garipov, T., Vetrov, D. P., and Wilson, A. G. (2019). A simple baseline for Bayesian uncertainty in deep learning. In *Advances in Neural Information Processing Systems*.
- Ng, A. and Jordan, M. (2001). On discriminative vs. generative classifiers: A comparison of logistic regression and naive Bayes. In *Advances in Neural Information Processing Systems*.
- Nocedal, J. and Wright, S. J. (1999). *Numerical Optimization*. Springer.
- Ovadia, Y., Fertig, E., Ren, J., Nado, Z., Sculley, D., Nowozin, S., Dillon, J., Lakshminarayanan, B., and Snoek, J. (2019). Can you trust your model’s uncertainty? evaluating predictive uncertainty under dataset shift. In *Advances in Neural Information Processing Systems*.
- Park, S., Bastani, O., Weimer, J., and Lee, I. (2020). Calibrated prediction with covariate shift via unsupervised domain adaptation. In *International Conference on Artificial Intelligence and Statistics*.
- Park, S., Dobriban, E., Lee, I., and Bastani, O. (2022). PAC prediction sets under covariate shift. In *International Conference on Learning Representations*.
- Peng, X., Usman, B., Kaushik, N., Hoffman, J., Wang, D., and Saenko, K. (2017). Visda: The visual domain adaptation challenge. *arXiv preprint arXiv:1710.06924*.
- Popoviciu, T. (1965). Sur certaines inégalités qui caractérisent les fonctions convexes. *Analele Stiintifice Univ. “Al. I. Cuza”, Iasi, Sectia Mat*, 11:155–164.
- Rahaman, R. et al. (2021). Uncertainty quantification and deep ensembles. In *Advances in Neural Information Processing Systems*.
- Recht, B., Roelofs, R., Schmidt, L., and Shankar, V. (2019). Do imagenet classifiers generalize to imagenet? In *International Conference on Machine Learning*.
- Russakovsky, O., Deng, J., Su, H., Krause, J., Satheesh, S., Ma, S., Huang, Z., Karpathy, A., Khosla, A., Bernstein, M., et al. (2015). Imagenet large scale visual recognition challenge. *International Journal of Computer Vision*, 115:211–252.
- Salvador, T., Voleti, V., Iannantuono, A., and Oberman, A. (2021). Frustratingly easy uncertainty estimation for distribution shift. *arXiv preprint arXiv:2106.03762*.
- Sensoy, M., Kaplan, L., and Kandemir, M. (2018). Evidential deep learning to quantify classification uncertainty. In *Advances in Neural Information Processing Systems*.
- Sharma, R., Gupta, M., and Kapoor, G. (2010). Some better bounds on the variance with applications. *Journal of Mathematical Inequalities*, 4(3):355–363.
- Solaiman, I., Brundage, M., Clark, J., Askill, A., Herbert-Voss, A., Wu, J., Radford, A., Krueger, G., Kim, J. W., Kreps, S., et al. (2019). Release strategies and the social impacts of language models. *arXiv preprint arXiv:1908.09203*.
- Stone, M. (1977). Asymptotics for and against cross-validation. *Biometrika*, pages 29–35.
- Sugiyama, M., Krauledat, M., and Müller, K.-R. (2007). Covariate shift adaptation by importance weighted cross validation. *Journal of Machine Learning Research*, 8(5).
- Thulin, M. (2014). The cost of using exact confidence intervals for a binomial proportion. *Electronic Journal of Statistics*, 8:817–840.
- Tishby, N., Pereira, F. C., and Bialek, W. (2000). The information bottleneck method. *arXiv preprint physics/0004057*.
- Tishby, N. and Zaslavsky, N. (2015). Deep learning and the information bottleneck principle. In *2015 IEEE Information Theory Workshop (itw)*, pages 1–5.
- Tu, Z. (2007). Learning generative models via discriminative approaches. In *IEEE Conference on Computer*

- Venkateswara, H., Eusebio, J., Chakraborty, S., and Panchanathan, S. (2017). Deep hashing network for unsupervised domain adaptation. In *IEEE Conference on Computer Vision and Pattern Recognition*.
- Virtanen, P., Gommers, R., Oliphant, T. E., Haberland, M., Reddy, T., Cournapeau, D., Burovski, E., Peterson, P., Weckesser, W., Bright, J., van der Walt, S. J., Brett, M., Wilson, J., Millman, K. J., Mayorov, N., Nelson, A. R. J., Jones, E., Kern, R., Larson, E., Carey, C. J., Polat, İ., Feng, Y., Moore, E. W., VanderPlas, J., Laxalde, D., Perktold, J., Cimrman, R., Henriksen, I., Quintero, E. A., Harris, C. R., Archibald, A. M., Ribeiro, A. H., Pedregosa, F., van Mulbregt, P., and SciPy 1.0 Contributors (2020). SciPy 1.0: Fundamental Algorithms for Scientific Computing in Python. *Nature Methods*, 17:261–272.
- Wang, X., Long, M., Wang, J., and Jordan, M. (2020). Transferable calibration with lower bias and variance in domain adaptation. In *Advances in Neural Information Processing Systems*.
- You, K., Wang, X., Long, M., and Jordan, M. (2019). Towards accurate model selection in deep unsupervised domain adaptation. In *International Conference on Machine Learning*.
- Yu, Y., Bates, S., Ma, Y., and Jordan, M. (2022). Robust calibration with multi-domain temperature scaling. In *Advances in Neural Information Processing Systems*.
- Zhang, Y., Liu, T., Long, M., and Jordan, M. (2019). Bridging theory and algorithm for domain adaptation. In *International Conference on Machine Learning*.

A Proof of claims

A.1 Non-convexity of the optimization problem

Let $\mathcal{G}_n(\mathcal{D}_S) := \{(x_k, y_k) \in \mathcal{D}_S : x_k \in \mathcal{G}_n\}$ and $\mathcal{G}_n(\mathcal{D}_T) := \{x_k \in \mathcal{D}_T : x_k \in \mathcal{G}_n\}$ for $n \in [M]$. By elementary algebra, we obtain the following

$$\hat{\alpha}_S^{(IW)}(\mathcal{G}_n; \{w_i\}_{i \in [B]}) = \left(\frac{1}{|\mathcal{G}_n(\mathcal{D}_T)|} \sum_{(x,y) \in \mathcal{G}_n(\mathcal{D}_T)} \frac{1}{w(x)} \right) \left(\frac{1}{|\mathcal{G}_n(\mathcal{D}_S)|} \sum_{x \in \mathcal{G}_n(\mathcal{D}_S)} \mathbf{1}(y = \hat{Y}(x))w(x) \right) \quad (18)$$

$$= \left(\frac{1}{|\mathcal{G}_n(\mathcal{D}_T)|} \sum_{i=1}^B \frac{a_i}{w_i} \right) \left(\frac{1}{|\mathcal{G}_n(\mathcal{D}_S)|} \sum_{i=1}^B b_i w_i \right) \quad (19)$$

where $a_i = |\mathcal{G}_n(\mathcal{D}_T) \cap \mathcal{B}_i|$ and $b_i = |\{(x_k, y_k) \in \mathcal{G}_n(\mathcal{D}_S) \cap \mathcal{B}_i | y_k = \hat{Y}(x_k)\}|$. Therefore, $\hat{\alpha}_S^{(IW)}(\mathcal{G}_n; \{w_i\}_{i \in [B]})$ is non-convex with respect to w_i for $i \in [B]$.

A.2 Proof of Proposition 4.1

Proof. By applying the triangle inequalities, we get the following inequality:

$$\begin{aligned} |\alpha_S(\mathcal{G}_n; w^*) - \alpha_S(\mathcal{G}_n; w^\dagger(n))| &\leq |\alpha_S(\mathcal{G}_n; w^*) - \hat{\alpha}_S^{(MC)}(\mathcal{G}_n)| + |\hat{\alpha}_S^{(MC)}(\mathcal{G}_n) - \hat{\alpha}_S^{(IW)}(\mathcal{G}_n; w^\dagger(n))| \\ &\quad + |\hat{\alpha}_S^{(IW)}(\mathcal{G}_n; w^\dagger(n)) - \alpha_S^{(IW)}(\mathcal{G}_n; w^\dagger(n))| + |\alpha_S^{(IW)}(\mathcal{G}_n; w^\dagger(n)) - \alpha_S(\mathcal{G}_n; w^\dagger(n))|. \end{aligned} \quad (20)$$

Note that the first and third terms in the right hand side are coming from the Monte-Carlo approximation, so they can be bounded by $\mathcal{O}(\log(1/\tilde{\delta})/|\mathcal{D}_n^S|)$ with probability at least $1 - \tilde{\delta}$ based on a concentration inequality such as the Hoeffding’s inequality. Also, the second term is bounded by the optimization error $\epsilon_{opt}(w^\dagger(n))$. Therefore, it is enough to analyze the fourth term.

The fourth term is coming from the bias of $\mathbb{E}_{T_{Y|X}}[\mathbf{1}(Y(X) = \hat{Y}(X))] = \hat{\alpha}_T(\mathcal{G}_n; w^\dagger(n))$, which we refer

to as *the bias of the identical accuracy assumption*. It can be bounded by

$$|\alpha_S^{(IW)}(\mathcal{G}_n; w^\dagger(n)) - \alpha_S(\mathcal{G}_n; w^\dagger(n))| \quad (21)$$

$$= \frac{P(X_T \in \mathcal{G}_n)}{P(X_S \in \mathcal{G}_n)} \left| \mathbb{E}_{p_T} \left[\frac{\mathbf{1}(Y(X) = \hat{Y}(X)) - \hat{\alpha}_T(\mathcal{G}_n; w^\dagger(n))}{w^\dagger(n)(X)} \mid X \in \mathcal{G}_n \right] \right| \quad (22)$$

$$\leq \frac{P(X_T \in \mathcal{G}_n)}{P(X_S \in \mathcal{G}_n)} \left(\mathbb{E}_{p_T} \left[(\mathbf{1}(Y(X) = \hat{Y}(X)) - \hat{\alpha}_T(\mathcal{G}_n; w^\dagger(n)))^2 \mid X \in \mathcal{G}_n \right] \mathbb{E}_{p_T} \left[\frac{1}{w^\dagger(n)(X)^2} \mid X \in \mathcal{G}_n \right] \right)^{1/2} \quad (23)$$

$$\leq \frac{P(X_T \in \mathcal{G}_n)}{2P(X_S \in \mathcal{G}_n)} \left(\mathbb{E}_{p_T} \left[(\mathbf{1}(Y(X) = \hat{Y}(X)) - \hat{\alpha}_T(\mathcal{G}_n; w^\dagger(n)))^2 \mid X \in \mathcal{G}_n \right] + \mathbb{E}_{p_T} \left[\frac{1}{w^\dagger(n)(X)^2} \mid X \in \mathcal{G}_n \right] \right) \quad (24)$$

$$\leq \frac{P(X_T \in \mathcal{G}_n)}{2P(X_S \in \mathcal{G}_n)} \left(\mathbb{E}_{p_T} \left[(\mathbf{1}(Y = \hat{Y}) - \alpha_T(\mathcal{G}_n; w^*))^2 \mid \mathcal{G}_n \right] + \frac{1}{w^\dagger(n)^2} \right) \quad (25)$$

where (23) holds due to the Cauchy-Schwarz inequality, (24) holds due to the AM-GM inequality, and $w^\dagger(n) := \min_{i \in [2B]} \{w_i^\dagger(n)\}$. \square

A.3 Proof of Proposition 4.2

Proof. Based on the proof of Proposition 4.1, it is enough to decompose $\mathbb{E}_{p_T} \left(\mathbf{1}(Y(X) = \hat{Y}(X)) - \hat{\alpha}_T(\mathcal{G}_n) \right)^2$ as follows

$$\mathbb{E}_{p_T} \left(\mathbf{1}(Y(X) = \hat{Y}(X)) - \hat{\alpha}_T(\mathcal{G}_n) \right)^2 \quad (26)$$

$$= \mathbb{E}_{p_T} \left(\mathbf{1}(Y(X) = \hat{Y}(X)) - \alpha_T(\mathcal{G}_n; w^*) + \alpha_T(\mathcal{G}_n; w^*) - \hat{\alpha}_T(\mathcal{G}_n) \right)^2 \quad (27)$$

$$= \mathbb{E}_{p_T} \left[\left(\mathbf{1}(Y(X) = \hat{Y}(X)) - \alpha_T(\mathcal{G}_n; w^*) \right)^2 + (\alpha_T(\mathcal{G}_n; w^*) - \hat{\alpha}_T(\mathcal{G}_n))^2 \right] \quad (28)$$

$$= \mathbb{E}_{p_T} \left(\mathbf{1}(Y(X) = \hat{Y}(X)) - \alpha_T(\mathcal{G}_n; w^*) \right)^2 + (\alpha_T(\mathcal{G}_n; w^*) - \hat{\alpha}_T(\mathcal{G}_n))^2 \quad (29)$$

where (28) holds due to $\mathbb{E}_{T_X} \mathbb{E}_{T_{Y|X}} \left[(\mathbf{1}(Y(X) = \hat{Y}(X)) - \alpha_T(\mathcal{G}_n; w^*))(\alpha_T(\mathcal{G}_n; w^*) - \hat{\alpha}_T(\mathcal{G}_n)) \right] = 0$. \square

B Discussions

B.1 On idea of estimating group accuracy

Our idea of predicting group accuracy, instead of an expected accuracy for each sample, can be motivated by a bias and variance decomposition analysis. Suppose we are given samples $\{x_i\}_{i=1}^{N_n} \in \mathcal{G}_n$ and a classifier f . Let $\beta(x) := \mathbb{E}_{Y|X}[\mathbf{1}(Y(x) = f(x))]$ be an expected accuracy of a classifier f at x , which is our goal to estimate. Let $D = \{(x, y) | y \sim Y | x, x \in \mathcal{G}_n\}$ be random samples with the realization of a label, which is the case in most machine learning cases. Then, the observed accuracy is $\hat{\beta}(x) := \mathbf{1}(y = f(x)) = \beta(x) + \epsilon_x$ where ϵ_x is random noise with zero mean and variance σ^2 . Note that the random noise ϵ_x exists unless the label is a deterministic function of x . While this might be true in the raw input space, this is highly unlikely in the representation space where most estimations are usually performed unless the representation contains all information about the input random variable X conditional on the label random variable Y (cf. (Tishby et al., 2000; Tishby and Zaslavsky, 2015)).

In this setting, the expected mean-square error of an estimator $g(x)$ for $\beta(x)$ at $x_i \in \mathcal{G}_n$ with respect to the realization of a label $y_i \sim Y | x$ can be decomposed by

$$\mathbb{E}_{D, \epsilon} [(\hat{\beta}(x_i) - g(x_i))^2] = \text{Var}_D(g(x_i; D)) + (\text{Bias}_D(g(x_i; D)))^2 + \sigma_{x_i}^2 \quad (30)$$

where $\text{Var}_D(g(x_i; D)) := \mathbb{E}_D[(g(x_i; D) - \mathbb{E}_D[g(x_i; D)])^2]$ is the variance of the estimator and $\text{Bias}_D(g(x_i; D)) := \mathbb{E}_D[g(x_i; D)] - \beta(x)$ is the bias of the estimator.

With the bias-variance decomposition in (30), we compare two maximum likelihood estimators (MLEs) where one predicts the expected accuracy at each x_i for $i \in [N_n]$ and the other one predicts the group accuracy for all x_i for $i \in [N_n]$ in terms of the expected mean-square accuracy estimation error.

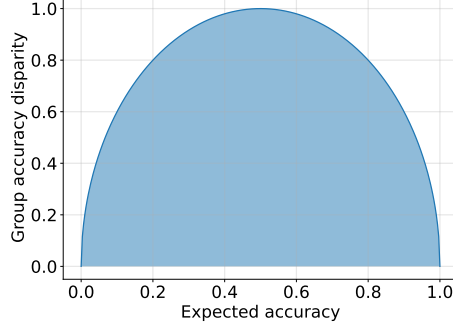


Figure A1: The shaded area includes values of group accuracy disparity satisfying the sufficient condition that the group accuracy estimator g_2 outperforms the individual group accuracy estimator g_1 .

Individual accuracy estimator: Let $g_1(x; D)$ be an estimator that predicts an accuracy at sample x given D . For this case, an MLE estimator is $g_1(x) = \hat{\beta}(x)$, which is unbiased because $\mathbb{E}_D(g_1(x; D)) = \beta(x)$ for each $x \in \mathcal{G}_n$. Therefore, this estimator has the average of expected errors

$$\frac{1}{N_n} \sum_{k=1}^{N_n} \mathbb{E}_{D, \epsilon} [(\hat{\beta}(x_k) - g_1(x_k; D))^2] = \bar{\sigma}^2 + \bar{\sigma}^2 \quad (31)$$

where $\bar{\sigma}^2 := \frac{1}{N_n} \sum_{i=1}^{N_n} \sigma_{x_i}^2$.

Group accuracy estimator: Let $g_2(x; D)$ be a group accuracy estimator that predicts the same group accuracy estimate for all $x \in \mathcal{G}_n$. An MLE estimator can be defined by $g_2(x; D) = \frac{1}{N_n} \sum_{i=1}^{N_n} \hat{\beta}(x_i)$, which is a biased estimator because $\mathbb{E}_D(g_2(x; D)) = \frac{1}{N_n} \sum_{i=1}^{N_n} \beta(x_i)$ for each $x \in \mathcal{G}_n$. Therefore, this estimator has the average of expected errors

$$\frac{1}{N_n} \sum_{k=1}^{N_n} \mathbb{E}_{D, \epsilon} [(\hat{\beta}(x_k) - g_2(x_k))^2] = \frac{1}{N_n} \bar{\sigma}^2 + \frac{1}{N_n} \sum_{k=1}^{N_n} \left(\frac{1}{N_n} \sum_{i=1}^{N_n} \beta(x_i) - \beta(x_k) \right)^2 + \bar{\sigma}^2 \quad (32)$$

$$= \frac{1}{N_n} \bar{\sigma}^2 + \text{Var}(\beta; D) + \bar{\sigma}^2 \quad (33)$$

where $\text{Var}(\beta; D)$ is the variance of the accuracy in group \mathcal{G}_n .

Comparison of the two estimators: The Popoviciu's inequality (Popoviciu, 1965) provides a sufficient condition for the group accuracy estimator g_2 to have a lower expected mean-squared error than the individual accuracy estimator g_1 as follows:

$$\frac{1}{4} \left(\max_{x' \in \mathcal{G}_n} \beta(x') - \min_{x' \in \mathcal{G}_n} \beta(x') \right)^2 \leq \frac{N_n - 1}{N_n} \bar{\sigma}^2 = \frac{N_n - 1}{N_n} \left(\frac{1}{N_n} \sum_{i=1}^{N_n} \beta(x_i)(1 - \beta(x_i)) \right) \quad (34)$$

where the equality comes from $\bar{\sigma}^2 = \frac{1}{N_n} \sum_{i=1}^{N_n} \sigma_{x_i}^2$ with $\sigma_{x_i}^2$ is the variance of the Bernoulli distribution with a parameter $\beta(x_i)$.

Recall that $\bar{\sigma}^2$ is due to the realization of only a single label at each sample, so it cannot be controlled unless we gather more labels of x_i or removing the stochasticity of a label by learning the perfect representation. However, we can reduce the term $\max_{x \in \mathcal{G}_n} \beta(x) - \min_{x \in \mathcal{G}_n} \beta(x)$ by constructing a group in a creative way discussed in Section 4.2. We also note that the sufficient condition is somewhat loose as we can see in Figure A1, which means that the group accuracy estimator could be better than the individual accuracy estimator in various cases. We finally note that the inequality can be further sharpened, i.e., the sufficient condition can be further relaxed, with tighter upper bounds of the variance (Bhatia and Davis, 2000; Sharma et al., 2010).

B.2 On choice of non-parametric estimators

Our concept of determining the IW from its CI can be applied with any other valid CI estimators. For example, by analyzing a CI of the odds ratio of the logistic regression used as a domain classifier (Bickel et al., 2007; Park et al., 2020; Salvador et al., 2021), a CI of the IW can be obtained. Then, IW-GAE can be applied in the same way as developed in Section 4. In this regard, advancements in IW estimation or CI estimation would be beneficial for accurately estimating the group accuracy, thereby model selection and uncertainty estimation. Therefore, we leave combining IW-GAE with advanced IW estimation techniques as an important future direction of research.

B.3 On choice of the number of groups

In this work, we estimate the group accuracy by grouping predictions based on the confidence of the prediction. Therefore, a natural question to ask is how to select the number of groups. If we use a small number of groups, then there would be high $IdentBias(w^\dagger; \mathcal{G}_n)$ because of the large variance of prediction correctness within a group. In addition, reporting the same accuracy estimate for a large number of predictions could be inaccurate in terms of representing uncertainty for individual predictions. Conversely, if we use a large number of bins, there would be high Monte-Carlo approximation errors, ϵ_{stat} . Therefore, it would result in a loose connection between the source group accuracy estimation error and the objective in the optimization problem (cf. Proposition 4.1). Therefore, it is important to choose a proper number of bins.

C Additional details

C.1 The nested optimization problem under the temperature scaling in the target domain

$$(t^\dagger, w^\dagger(n)) \in \arg \min_{t \in \mathcal{T}} \arg \min_{\{w_i^{(S)}, w_i^{(T)}\}_{i \in [B]}} \left(\hat{\alpha}_S^{(MC)}(\mathcal{G}_n) - \hat{\alpha}_S^{(IW)}(\mathcal{G}_n; \{w_i^{(S)}, w_i^{(T)}\}_{i \in [B]}) \right)^2 \quad (35)$$

$$\text{s.t. } w_i^{(S)} \in \Phi_i, \quad \text{for } i \in [B] \quad (36)$$

$$w_i^{(T)} \in \Phi_i, \quad \text{for } i \in [B] \quad (37)$$

$$\|w_i^{(T)} - w_i^{(S)}\|_2^2 \leq \delta^{(tol)} \quad \text{for } i \in [B] \quad (38)$$

$$\left| \hat{\mathbb{E}}_{p_S}[\tilde{w}^{(S)}(X)|X \in \mathcal{G}_n] - \frac{\hat{P}(X_T \in \mathcal{G}_n^{(t)})}{\hat{P}(X_S \in \mathcal{G}_n)} \right| \leq \delta^{(prob)} \quad (39)$$

$$\left| \hat{\mathbb{E}}_{p_T}[1/\tilde{w}^{(T)}(X)|X \in \mathcal{G}_n^{(t)}] - \frac{\hat{P}(X_S \in \mathcal{G}_n)}{\hat{P}(X_T \in \mathcal{G}_n^{(t)})} \right| \leq \delta^{(prob)} \quad (40)$$

In the above optimization problem, we note that temperature scaling also changes the IW based estimator by

$$\hat{\alpha}_S^{(IW)}(\mathcal{G}_n; \{w_i^{(S)}, w_i^{(T)}\}_{i \in [B]}) = \hat{\mathbb{E}}_{p_T} \left[\frac{1}{\tilde{w}^{(T)}(X)} \middle| X \in \mathcal{G}_n^{(t)} \right] \hat{\mathbb{E}}_{p_S} \left[\mathbf{1}(Y = \hat{Y}) \tilde{w}^{(S)}(X) \middle| X \in \mathcal{G}_n \right]. \quad (41)$$

D Experimental details

We follow the exact same training configurations as those used in the Transfer Learning Library, except we separate 20% as the validation dataset from the source domain (in the original implementation, validation is performed with the test dataset for Office-Home).

The configuration of training MDD for Office-Home is as follows: MDD is trained for 30 epochs with SGD with momentum parameter 0.9 and weight decay of 0.0005. The learning rate is schedule by $\alpha \cdot (1 + \gamma \cdot t)^{-\eta}$ where t is the iteration counter, $\alpha = 0.004$, $\gamma = 0.0002$, $\eta = 0.75$, and the stochastic gradient is computed with minibatch of 32 samples from the source domain and 32 samples from the target domain. Also, it uses the margin coefficient of 4 as the MDD-specific hyperparameter. For the model architecture, it uses ResNet-50 pre-trained on ImageNet (Russakovsky et al., 2015) with the bottleneck dimension of 2,048.

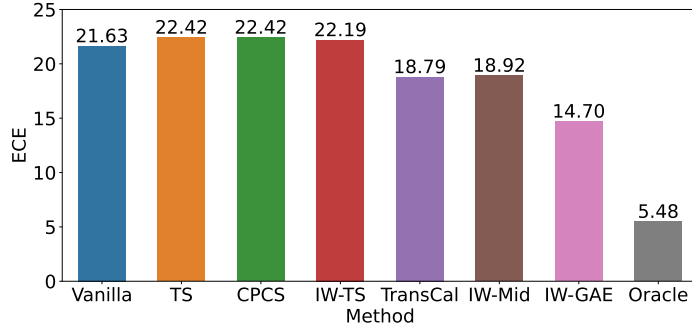


Figure A2: Large-scale model calibration benchmark result of MDD with ResNet-101 on VisDA 2017. The numbers indicates the mean ECE across ten repetitions with boldface for the minimum mean ECE.

IW-GAE specific details For CI estimation, we follow the same configuration with the original method (Park et al., 2022). Specifically, we use constant $G = 0.001$, CI level $\bar{\delta} = 0.05$, and the number of bins $B = 10$. In addition, we use the maximum IW value $\bar{M} = 6.0$ and the minimum IW value $w^\dagger(n) = 1/6$ for $n \in [M]$ for tightening the upper bounds in (5) and (15) (cf. Section 4.1).

In addition, for IW-GAE, we use the constraint relaxation constants $\delta^{(tol)} = 0.1$ and $\delta^{(prob)} = 0.3$. We also use the number of accuracy group $M = 10$ and analyze the sensitivity for M in Appendix E.6. For implementing sequential least square programming, we use the SciPy Library (Virtanen et al., 2020) with tolerance 10^{-8} that is used to check a convergence condition (other optimizer-specific values follow the default values in SciPy) and choose the middle points from CIs of binned IW as an initial solution. For nested optimization, we set $\mathcal{T} := \{0.85, 0.90, 0.95, 1.00, 1.05, 1.10\}$.

E Additional experiments

E.1 Large-scale image classification task

We perform an additional large-scale experiment with the VisDA-2017 (Peng et al., 2017) containing around 280,000 images of 12 categories from two domains (real and synthetic images). For this experiment, we use ResNet-101 with the bottleneck dimension of 1,024, following the default setting in the Transfer Learning Library. All other configurations are the same as the training configuration of the Office-Home dataset (cf. Appendix D). Figure A2 represents the result of the VisDa-2017 experiment, which shows that the IW-GAE achieves the best performance among all baselines. Specifically, IW-GAE reduces the ECE of the state-of-the-art (TransCal) by 21%. We note that the IW-Mid achieves a comparable performance with TransCal, unlike the OfficeHome experiment. This result could be explained by an accurate CI estimation under a large number of samples. We leave analyzing the impacts of the number of samples on the CI estimation and the performance of IW-GAE as an important future direction of research, which could provide a strategy for choosing which CI estimator to use under which condition.

E.2 CDAN

In this section, we perform additional experiments with the conditional domain adversarial network (Long et al., 2018) which is also a popular UDA method. As in the experiments with MDD, we use ResNet-50 as the backbone network and OfficeHome as the dataset. The learning rate schedule for CDAN is $\alpha \cdot (1 + \gamma \cdot t)^{-\eta}$ where t is the iteration counter, $\alpha = 0.01$, $\gamma = 0.001$, and $\eta = 0.75$. The remaining training configuration for CDAN is the same as the MDD training configuration except it uses the bottleneck dimension of 256 and weight decay of 0.0005 (cf. Appendix D). As we can see from Table A1, IW-GAE achieves the best performance among all considered methods, achieving the best ECE in 8 out of the 12 cases as well as the lowest mean ECE. We note that TransCal achieves a performance comparable to IW-GAE in this experiment, but considering the results in the other tasks, IW-GAE is still an appealing method for performing the model calibration task.

Method	Ar-Cl	Ar-Pr	Ar-Rw	Cl-Ar	Cl-Pr	Cl-Rw	Pr-Ar	Pr-Cl	Pr-Rw	Rw-Ar	Rw-Cl	Rw-Pr	Avg
Vanilla	30.73	18.38	14.37	25.63	22.44	19.10	27.54	36.72	12.48	19.93	31.12	10.88	22.44
TS	29.68	19.40	14.40	22.15	19.97	16.88	28.82	38.03	12.99	20.46	31.91	11.83	22.21
CPCS	18.78	18.09	14.74	22.18	20.74	16.33	29.30	34.92	11.92	20.99	31.41	11.07	20.87
IW-TS	12.38	16.79	14.85	21.75	20.06	16.92	29.30	38.84	13.30	20.82	31.10	11.37	20.62
TransCal	7.94	14.05	12.91	7.82	9.25	10.23	9.37	12.60	14.29	9.92	9.76	17.51	11.30
IW-Mid	36.05	47.70	26.82	21.08	22.95	21.55	18.88	28.99	15.39	21.16	28.16	25.27	26.17
IW-GAE	13.98	29.82	9.44	6.55	5.59	10.16	5.29	13.47	11.01	11.12	7.26	9.84	11.13
Oracle	7.91	8.80	6.05	7.57	7.93	6.76	9.07	9.14	4.04	7.16	9.19	5.65	7.44

Table A1: Model calibration benchmark results of CDAN with ResNet-50 on Office-Home. The numbers indicates the mean ECE across ten repetitions with boldface for the minimum mean ECE.

Method	Ar-Cl	Ar-Pr	Ar-Rw	Cl-Ar	Cl-Pr	Cl-Rw	Pr-Ar	Pr-Cl	Pr-Rw	Rw-Ar	Rw-Cl	Rw-Pr	Avg
Vanilla	47.22	74.14	77.76	61.85	70.96	71.59	60.98	53.63	78.93	71.57	57.04	83.96	67.47
IWCV	54.46	74.22	72.27	61.48	70.49	70.62	61.30	51.13	78.37	72.94	58.43	84.00	67.48
DEV	54.04	73.94	78.16	61.52	63.19	70.7	60.43	53.63	78.93	71.57	58.62	83.89	67.39
IW-Mid	54.04	72.63	78.37	62.05	71.28	71.45	61.25	54.39	79.07	73.19	58.75	80.06	68.04
IW-GAE	54.32	73.98	78.51	61.96	71.25	71.70	61.10	54.30	78.91	73.22	58.70	83.86	68.48
Lower bound	41.90	64.88	72.27	52.00	58.48	62.13	53.52	38.33	70.92	63.41	44.81	75.83	58.21
Oracle	54.80	74.79	78.61	62.46	71.59	72.18	61.64	54.64	79.44	73.42	59.43	84.12	68.93

Table A2: Checkpoint selection benchmark results of MDD with ResNet-50 on Office-Home. The numbers indicate the mean test accuracy of selected model across ten repetitions with boldface for the maximum mean test accuracy.

E.3 Checkpoint selection

In this section, we perform the task of choosing the best checkpoint during training for examining IW-GAE’s model selection performance. Specifically, we first train MDD on the OfficeHome dataset for 30 epochs and save the checkpoint at the end of each epoch. Then, we choose the best checkpoint based on IW-GAE and baselines described in Section 5.2. As shown in Table A2, the model selected based on IW-GAE achieves the best average test accuracy, which is consistent with the results in the hyperparameter selection task (cf. the model selection task in Table 1). Specifically, IW-GAE improves the second-best method (IWCV) by 9% and achieves the best checkpoint selection for 3 out of the 12 domains.

E.4 Qualitative evaluation of IW-GAE

To qualitatively analyze IW-GAE, we also visualize reliability curves that compare the estimated group accuracy with the average accuracy in Figure A3. We first note that IW-GAE tends to accurately estimate the true group accuracy for most groups under different cases compared to IW-Mid. The accurate group accuracy estimation behavior of IW-GAE explains the results that the IW-GAE improves IW-Mid for most cases in the model calibration and selection tasks (cf. Table 1). For most cases, true accuracy is in between the lower and upper IW estimators, albeit the interval length tends to increase for high-confidence groups. This means that the CI of the IW based on the Clopper-Pearson method successfully captures the IW in the CI. We also note that the true accuracy is close to the lower IW estimator in the lower confidence group and the middle IW estimator in the high confidence group. An observation that the true accuracy’s relative positions in CIs varies from one group to another group motivates why an adaptive selection of binned IWs as ours is needed.

E.5 Ablation study

In this section, we perform an ablation study of our key design choices for group construction (cf. Section 4.2). The first ablation study examines group construction based on the maximum value of the softmax output by constructing a group function based on IW. The second ablation study examines the effectiveness of our nested optimization with temperature scaling (cf. Section 4.2), by excluding the outer optimization in the nested optimization; i.e., setting $\mathcal{T} = \{1\}$ in Appendix C.1. Specifically, we repeat the model calibration experiment with MDD on four randomly selected domains in the OfficeHome dataset (Ar-Pr, Pr-Cl, Rw-Cl, Rw-Pr).

Table A3 presents the results of the ablation study. First, note that the grouping by the maximum value of softmax significantly impacts the performance of IW-GAE. If we assume the group accuracy

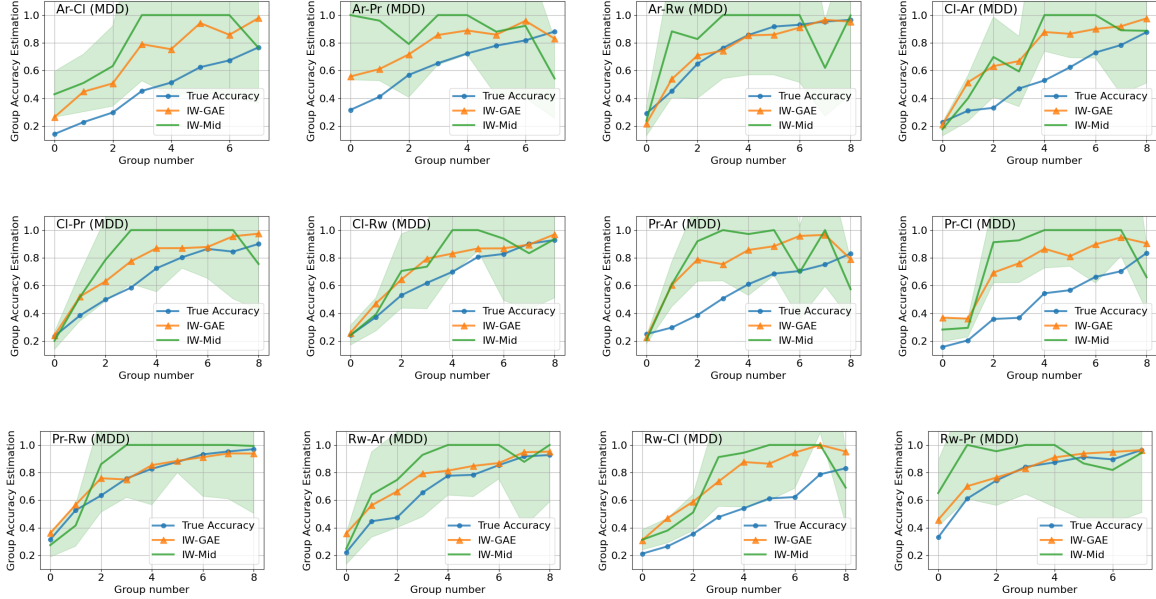


Figure A3: True group accuracy and estimated group accuracy of IW-GAE and IW-Mid under MDD. The shaded areas represent possible group accuracy estimation with binned IWs in the CI. The title of a figure represents “Source-Target.” For IW-Mid and IW-GAE, we clip the accuracy estimations when they exceed 1, which can occur when the upper bound of CI is large. Also, the number of groups in the figure is different for some domains because there can be a group that contains no target samples (we set $M = 10$ for all cases).

Method	Ar-Pr	Pr-CI	Rw-CI	Rw-Pr	Avg
IW-GAE w/ grouping by IW and w/o the nested optimization	15.07	36.02	35.01	5.23	22.83
IW-GAE w/ grouping by IW	14.18	34.67	35.08	5.30	22.31
IW-GAE w/o the nested optimization	11.43	16.57	9.38	5.91	10.82
IW-GAE	4.70	17.49	9.52	8.14	9.97

Table A3: An ablation study of key design choices of constructing a group by the maximum value of the softmax and using nested optimization with temperature scaling on the target domain for IW-GAE. We use MDD with ResNet-50 on Office-Home. The numbers indicate the mean ECE across ten repetitions.

estimation ability of IW-GAE is not significantly reduced after changing the grouping function $I^{(g)}$, the reduction in the performance could be due to a large variance of prediction accuracy within a group (cf. the case of group 2 in Figure 1(b)). Specifically, the large value of $\text{Var}(\mathbf{1}(Y = \hat{Y})|\mathcal{G}_n)$ increases the $\text{IdentBias}(w^\dagger(n); \mathcal{G}_n)$, which can loosen the upper bound of the source group accuracy estimation error in (15). Given its significant impact on the calibration performance, we want to remark few challenging aspects of developing an ideal group function for future work. Specifically, note that the core factor in $\text{IdentBias}(w^\dagger(n); \mathcal{G}_n)$ impacted by $I^{(g)}$ is $\text{Var}(\mathbf{1}(Y = \hat{Y})|\mathcal{G}_n)$. This term depends on the labeled information in the target domain, so it is hard to foretell changes in $\text{IdentBias}(w^\dagger(n); \mathcal{G}_n)$ as we change $I^{(g)}$. Furthermore, even if we have a labeled dataset in the target domain, finding the optimal $I^{(g)}$ that minimizes $\text{IdentBias}(w^\dagger(n); \mathcal{G}_n)$ is a combinatorial optimization problem, which is one of the most challenging optimization problems.

Next, note that nested optimization results in improvement of the ECE on average but it is effective only in four out of eight cases. This is surprising because the nested optimization problem is guaranteed to reduce $\epsilon_{opt}(w^\dagger(n))$ as \mathcal{T} contains the case that corresponds to the setting without the nested optimization; $1 \in \mathcal{T}$. This motivates our further investigation of the relationship between $\epsilon_{opt}(w^\dagger(n))$ and $\text{IdentBias}(w^\dagger(n); \mathcal{G}_n)$ in Appendix E.7. In a nutshell, we found the cases when reducing $\epsilon_{opt}(w^\dagger(n))$ increases $\text{IdentBias}(w^\dagger(n); \mathcal{G}_n)$. Therefore, it can increase the upper bound of a source group accuracy estimation error in (15). We also found a (weak) correlation between $\epsilon_{opt}(w^\dagger(n))$ and $\text{IdentBias}(w^\dagger(n); \mathcal{G}_n)$, which can explain the average improvement by the nested optimization problem. We present more details in Appendix E.7.

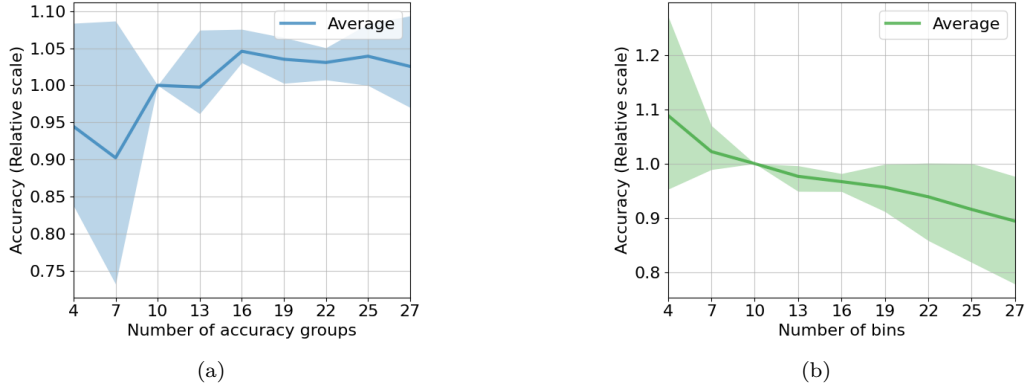


Figure A4: Sensitivity analysis of IW-GAE with respect to the number of groups M and the number of bins B (b) on four domains (Ar-Pr, Pr-Cl, Rw-Cl, Rw-Pr) in the OfficeHome dataset. Default hyperparameters for M and B are 10, and we normalize the accuracy for each domain by its performance under the default hyperparameters. Average represents the average relative accuracy for each value of the hyperparameter and the shaded areas represent areas between the minimum and the maximum relative accuracy over the 4 domains.

E.6 Sensitivity analysis

In this section, we conduct a sensitivity analysis with respect to our key hyperparameters of the number of accuracy groups M and the number of bins B . As in the ablation study in Appendix E.5, we perform the model calibration experiment with MDD on the four domains in the OfficeHome dataset (Ar-Pr, Pr-Cl, Rw-Cl, Rw-Pr). Figure A4 shows the sensitivity analysis results with hyperparameter values $M \in [4, 27]$ and $B \in [4, 27]$ (the default value for both M and B is 10). Within the search space, the average performances do not change more than 10%, which means that IW-GAE would outperform state-of-the-art (cf. Table 1) also under such altered settings. Also, we can see that the performance changes under different hyperparameter values are somewhat stable; the maximum and minimum changes are within the range of 10% for most cases, even though a large variance in the performances appears for extreme values such as $M = 4$, $B = 4$, and $B = 27$. The results show the robustness of IW-GAE with respect to small changes in the key hyperparameter values.

E.7 Analysis of $\epsilon_{opt}(w^\dagger(n))$ and $IdentBias(w^\dagger(n); \mathcal{G}_n)$ of IW and their relation to source and target group accuracy estimation errors

In this section, we aim to answer the following question about the central idea of this work: “Does solving the optimization problem in (9)-(14) result in an accurate target group accuracy estimator?” Specifically, we analyze the relationship between the optimization error $\epsilon_{opt}(w^\dagger(n))$, the bias of the identical accuracy assumption $IdentBias(w^\dagger(n); \mathcal{G}_n)$, the source group accuracy estimation error $|\alpha_S(\mathcal{G}_n; w^*) - \alpha_S(\mathcal{G}_n; w^\dagger(n))|$, and the target group accuracy estimation error $|\alpha_T(\mathcal{G}_n; w^*) - \alpha_T(\mathcal{G}_n; w^\dagger(n))|$ from the perspective of (5) and (15)². To this end, we gather $w^\dagger(n)$ obtained by solving the optimization problem under all temperature parameters in the search space $t \in \mathcal{T}$ with MDD on the OfficeHome dataset (720 IWs from 6 values of the temperature parameter, 12 cases, and 10 groups). Then, by using the test dataset in the source and the target domains, we obtain the following observations.

In (5), we show that $|\alpha_T(\mathcal{G}_n; w^*) - \alpha_T(\mathcal{G}_n; w^\dagger(n))|$ is upper bounded by $|\alpha_S(\mathcal{G}_n; w^*) - \alpha_S(\mathcal{G}_n; w^\dagger(n))|$. However, the inequality could be loose since the inequality is obtained by taking the maximum over the IW values. Considering that the optimization problem is formulated for finding $w^\dagger(n)$ that achieves small $|\alpha_S(\mathcal{G}_n; w^*) - \alpha_S(\mathcal{G}_n; w^\dagger(n))|$ (cf. Proposition 4.1), the loose connection between the source and target group accuracy estimation errors can potentially enlighten a fundamental difficulty to our approach. However, as we can see from Figure A5, it turns out that $|\alpha_S(\mathcal{G}_n; w^*) - \alpha_S(\mathcal{G}_n; w^\dagger(n))|$ is strongly correlated with $|\alpha_T(\mathcal{G}_n; w^*) - \alpha_T(\mathcal{G}_n; w^\dagger(n))|$. This result validates our approach of reducing the source accuracy estimation error of the IW-based estimator for obtaining an accurate group accuracy estimator in the

²Technically speaking, the computed values in this experiment are the empirical expectation which can contain a statistical error. However, since we have no access to the data generating distribution, we perform the analysis as if these values are the population expectations.

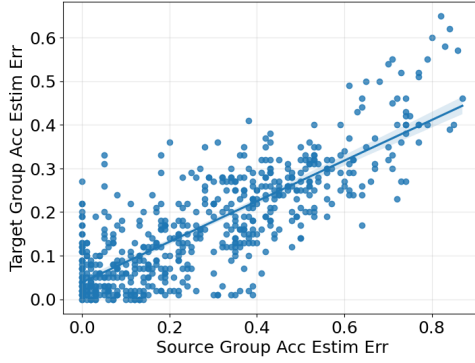


Figure A5: The relationship between source and target group accuracy estimation errors.

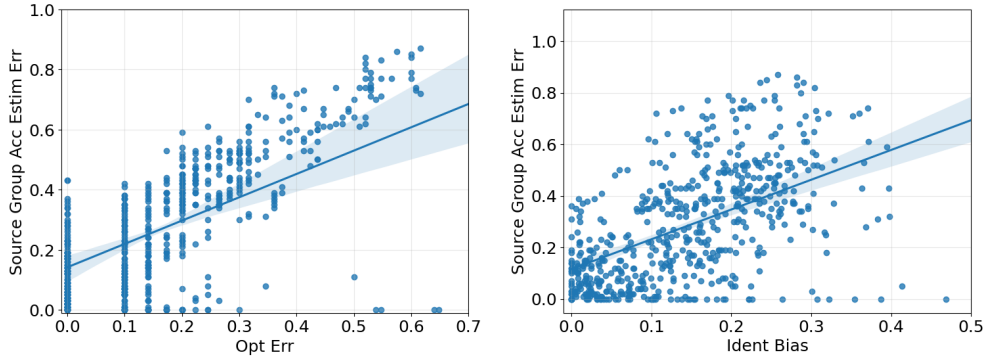


Figure A6: The relationship between $\epsilon_{opt}(w^\dagger(n))$ and the source group accuracy estimation error (left) and the relationship between $IdentBias(w^\dagger(n); \mathcal{G}_n)$ and the source group accuracy estimation error (right).

target domain.

In (15), we show that $|\alpha_S(\mathcal{G}_n; w^*) - \alpha_S(\mathcal{G}_n; w^\dagger(n))| \leq \epsilon_{opt}(w^\dagger(n)) + \epsilon_{stat} + IdentBias(w^\dagger(n); \mathcal{G}_n)$, which motivates us to solve the optimization problem for reducing $\epsilon_{opt}(w^\dagger(n))$ (cf. Section 4.1) and to construct groups based on the maximum value of softmax for reducing $IdentBias(w^\dagger(n); \mathcal{G}_n)$ (cf. Section 4.2). Again, if these terms are loosely connected to $|\alpha_S(\mathcal{G}_n; w^*) - \alpha_S(\mathcal{G}_n; w^\dagger(n))|$, a fundamental difficulty arises for our approach. In this regard, we analyze the relationship between $\epsilon_{opt}(w^\dagger(n))$, $IdentBias(w^\dagger(n); \mathcal{G}_n)$, and $|\alpha_S(\mathcal{G}_n; w^*) - \alpha_S(\mathcal{G}_n; w^\dagger(n))|$. From Figure A6, we can see that both $\epsilon_{opt}(w^\dagger(n))$ and $IdentBias(w^\dagger(n); \mathcal{G}_n)$ are strongly correlated to the source group accuracy estimation error. Combined with the observation in Figure A5, this observation explains the impressive performance gains by IW-GAE developed for reducing $\epsilon_{opt}(w^\dagger(n))$ and $IdentBias(w^\dagger(n); \mathcal{G}_n)$.

Next, we analyze the efficacy of solving the optimization problem for obtaining an accurate target group accuracy estimator. To this end, we analyze the relationship between $\epsilon_{opt}(w^\dagger(n))$ and $|\alpha_T(\mathcal{G}_n; w^*) - \alpha_T(\mathcal{G}_n; w^\dagger(n))|$. From Figure A7, $\epsilon_{opt}(w^\dagger(n))$ is correlated with $|\alpha_T(\mathcal{G}_n; w^*) - \alpha_T(\mathcal{G}_n; w^\dagger(n))|$, which explains the performance gains in the model calibration and selection tasks by IW-GAE. However, the correlation is weaker than the cases analyzed in Figure A5 and Figure A6. We conjecture that this is because $\epsilon_{opt}(w^\dagger(n))$ is connected to $|\alpha_T(\mathcal{G}_n; w^*) - \alpha_T(\mathcal{G}_n; w^\dagger(n))|$ through two inequalities (5) and (15), and this results in a somewhat loose connection between $\epsilon_{opt}(w^\dagger(n))$ and $|\alpha_T(\mathcal{G}_n; w^*) - \alpha_T(\mathcal{G}_n; w^\dagger(n))|$.

In Figure A7, we also note that the optimization problem is subject to a non-identifiability issue that the solutions with the same optimization error can have significantly different target group accuracy estimation errors (e.g., points achieving the zero optimization error in Figure A7). We remark that the non-identifiability issue motivates an important future direction of research that develops a more sophisticated objective function and a regularization function that can distinguish estimators with different target group accuracy estimation errors.

Finally, we analyze the relationship between $\epsilon_{opt}(w^\dagger(n))$ and $IdentBias(w^\dagger(n); \mathcal{G}_n)$ in Figure A8. In general, we can see a weak correlation between $\epsilon_{opt}(w^\dagger(n))$ and $IdentBias(w^\dagger(n); \mathcal{G}_n)$. This means that, in general, finding a better solution in terms of $\epsilon_{opt}(w^\dagger(n))$ could also reduce $IdentBias(w^\dagger(n); \mathcal{G}_n)$.

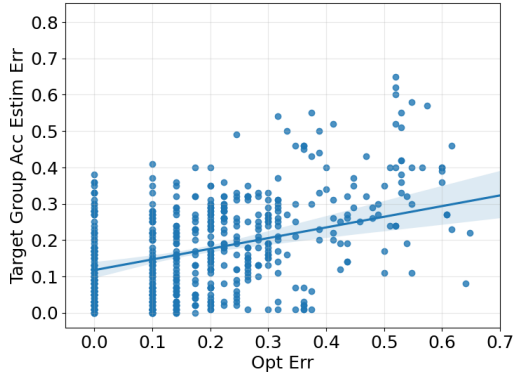


Figure A7: The relationship between $\epsilon_{opt}(w^\dagger(n))$ and the target group accuracy estimation error.

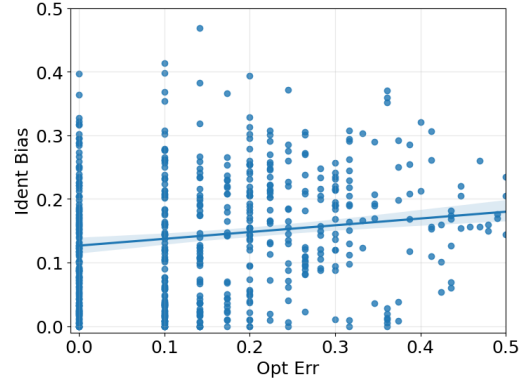


Figure A8: The relationship between $\epsilon_{opt}(w^\dagger(n))$ and $IdentBias(w^\dagger(n); \mathcal{G}_n)$.

However, there are many cases in which different IWs have the same $\epsilon_{opt}(w^\dagger(n))$ but significantly different $IdentBias(w^\dagger(n); \mathcal{G}_n)$. Furthermore, reducing $\epsilon_{opt}(w^\dagger(n))$ increases $IdentBias(w^\dagger(n); \mathcal{G}_n)$ for some cases. This observation explains small performance gains by the nested optimization problem as seen in the ablation study (cf. Appendix E.5).